TEMPORAL REFINEMENT OF WATER BUDGETS IN SMALL PACIFIC ISLAND DRAINAGE BASINS FROM DAILY RAINFALL AND TEMPERATURE MAPS

A THESIS SUBMITTED TO THE GRADUATE DIVISION OF THE
UNIVERSITY OF HAWAIʻI AT MĀNOA IN PARTIAL FULFILLMENT
OF THE REQUIREMENTS FOR THE DEGREE OF

MASTER OF SCIENCE
IN
EARTH AND PLANETARY SCIENCE
OCTOBER 2021

By
Theodore M. Brennis

Thesis Committee:
Nicole Lautze (Chairperson)
Robert Whittier
Abby Frazier

Keywords: groundwater recharge, water budgets, Hawaiʻi, evapotranspiration, quickflow, precipitation, drainage basin

ACKNOWLEDGEMENTS

First, I would like to thank my wife, Paige, for her support, patience, strength, encouragement, wisdom, and love through this exciting journey. You have been an absolute rock for our family, and I am so grateful to have you in my life . Thank you for all the grammar checks, the patience through late labs, the understanding during long nights and field days, and the cheerful, kind, gracious heart you have maintained through all these crazy changes. I love you more than I can express with words.

I would like to thank my graduate committee. To my committee chair, Nicole Lautze, thank you for investing so much time into my academic and personal growth. I could not have hoped for a better advisor and mentor. To Robert Whittier, and Abby Frazier, thank you for your mentorship and flexibility, and for lending your expertise so generously. It has been a pleasure working with you all, and I have learned so much from each of you.

To Diamond Tachera and Daniel Dores, thank you for the camaraderie, laughs, mentorship and friendship. I wish you both success in all your future endeavors and hope that our paths cross often.

I am grateful to both the EPSCoR ʻIke Wai and the DoD SMART programs for providing the financial support necessary to complete this project.

This undertaking would have been impossible without the fine instruction, training, and support I have received within the University of Hawaiʻi at Mānoa Department of Earth Sciences. I would especially like to thank Professors Scott Rowland, Thomas Shea, Neil Frazier, and Steve Martel for your amazing classes, and for so often cheerfully dropping everything you were doing to entertain my questions outside of office hours. To Lily Shao, Leona Anthony, Susan Van Gorder, Arlene Sullivan and all the other amazing staff within SOEST, thank you so much for all the support and guidance. Mahalo nui loa!

Lastly, and most importantly, I owe an unrepayable and humbling debt to my Lord and Savior Jesus Christ. His awesomeness has been on full display these last few years as I have studied His creation on these breathtaking islands in the Pacific. Even more amazing to me than His creative power is His unending patience, mercy, and kindness towards a completely underserving recipient (me). “For from Him and through Him and to Him are all things. To Him be the glory forever! Amen.” (Romans 11:36)

ABSTRACT

Understanding the movement, distribution, and replenishment of groundwater is critical to sustainably managing this vital resource in Hawai‘i, USA, where groundwater meets more than 90% of freshwater needs statewide. Geochemical methods have been used increasingly to understand and model groundwater flow, but these methods are limited by the resolution of recharge measurements and the availability of precipitation chemistry data. Recent increases in climate data availability in Hawai‘i allow water budgets to be examined with greater spatio-temporal resolution than ever before. While the current estimates of groundwater recharge are limited to annual long-term averages provided by the USGS, this paper provides a method for producing island-wide, monthly estimates of groundwater recharge using daily precipitation and temperature raster data. Recharge is calculated using a simple water budget: recharge ≈ precipitation – evapotranspiration – quickflow. Monthly precipitation, quickflow, evapotranspiration, and recharge are estimated for the island of O‘ahu between 1990 and 2014. Precipitation data are aggregated from recently published daily rainfall maps. Quickflow is calculated using simple regional regressions created by the USGS and compared with estimates from two different stream hydrograph baseflow separations. Evapotranspiration is calculated using a modification of the Thornthwaite equation, which was validated with local weather station data. The resulting estimates are compared with standards to quantitatively assess uncertainty and agreement. Our results show strong agreement with long-term average recharge estimates given by the USGS, and interannual climate trends further corroborate this agreement. These findings indicate that monthly estimates of groundwater recharge may be produced on O‘ahu via a low data intensity method with sufficient accuracy to better constrain recharge patterns for the island, and potentially improve groundwater management. These findings further suggest that the model presented here can be applied in any area where data on monthly precipitation, monthly temperature, and general quickflow trends are available.

TABLE OF CONTENTS

LIST OF TABLES

LIST OF FIGURES

1. Introduction

1.1 Purpose

This study provides a method to calculate island-wide monthly groundwater recharge using a simplified, easily reproducible technique that allows for thorough error analysis within the study area. Groundwater is a critical resource in Hawai‘i, USA, supplying 99% of the domestic water needs statewide (Gingerich and Oki, 2000), and more than 90% of domestic freshwater needs on the island of O‘ahu (Nichols et al. 1996). The need to calculate groundwater recharge in general to understand water availability is clear, however the need for monthly estimates of groundwater recharge is, perhaps, less tangible. This need stems in part from the growing use of geochemical methods to understand the movement and distribution of groundwater in Hawai‘i (Fackrell 2016; Scholl 1995; Scholl et al. 2002; Glenn et al., 2013). A key assumption in most geochemical groundwater studies is that the chemistry of precipitation is the same as, or approximately that of, groundwater recharge. Recent research has shown this is not the case. Several studies have highlighted the spatio-temporal heterogeneity and periodicity of precipitation chemistry in Hawai‘i (Booth et al., 2021; Tachera et al., 2021; Dores et al., 2020; Scholl, Eugster, & Burkard 2011; Scholl et al. 2007). Intuitively, groundwater recharge also changes in both time and space, with higher recharge generally occurring when and where precipitation is greatest (Dunne & Leopold 1978; Visher & Mink 1964). The natural consequence of this heterogeneity is local volume-weighted differences in recharge chemistry. Few studies have attempted to account for this chemical variability (Jasechko et al., 2011). Matters are complicated further when we consider the subsurface behavior of water. Since groundwater flows from a starting point (recharge) to an ending point (well, spring, aquifer, etc.), and since recharge can occur at each point along the entire groundwater flow path, the ending chemical composition for a conservative species will be the recharge volume-weighted average of the precipitation chemistry integrated along the whole flow path (Fackrell 2016; Scholl 1995; Kendall & McDonnell 1999). Any mixing model that does not account for this spatio-temporal heterogeneity in recharge chemistry will have limited accuracy. Linking groundwater chemistry with precipitation chemistry thus requires an understanding of the spatio-temporal heterogeneity of both precipitation chemistry and recharge volume. This study seeks to meet the latter requirement by producing monthly estimates of recharge for the island of O‘ahu.

1.2 Study Area Overview

This study was conducted on the island of O‘ahu, USA, the most populous and third largest island of the Hawaiian archipelago. O‘ahu lies between 21° and 22°N and 157° and 159°W. The island is formed from the remains of two extinct shield volcanoes, Wai‘anae (4.0 to 2.9 Ma) and the younger Ko‘olau (3.0 to 1.7 Ma) (Sherrod et al. 2007; Figure 1). Both volcanoes are composed of successive layers of lava flows interspersed locally with pyroclastic and sedimentary deposits, and both have at least two rift zones emanating from a summit caldera (Sherrod et al. 2007; Stearns et al. 1946; Izuka et al., 2018; Figure 2). Erosion and mass wasting events have created severe topography characterized by steep, deeply incised valleys radiating from mountainous highland which terminate in flat board scrublands that drape coastal plains in the south and southwest (Sherrod et al. 2007; Figure 1). In terms of climate, two general weather patterns dominate on O‘ahu. First, the Hawaiian Islands sit in the path of the northeast trade winds, which are a circulation pattern associated with the North Pacific High (Giambelluca 1983). The trade winds persist more than 90% of the time during summer months, and approximately 50% of the time during winter months. The trade winds create orographic precipitation in high elevation areas (Figure 2; Noguchi 1979; Wuhl 1935). Maximum mean annual rainfall exceeds 6,500 mm/year in the Ko‘olau range and 2,000 mm/year in the Wai‘anae range (Giambelluca et al. 2013). The second dominant weather pattern is atmospheric disturbance-based storms (Longman et al. 2021). In the absence of trade winds, subtropical cyclones can bring heavier, more evenly distributed rainfall. These events are focused in the winter months and occur sporadically yet can supply more than half the annual rainfall in the drier, leeward areas of O‘ahu (Giambelluca 1983; Dores et al. 2020). Across the island of O‘ahu, mean annual rainfall can vary from 500-6,500 mm/year over less than 20 miles (Giambelluca et al. 2013).

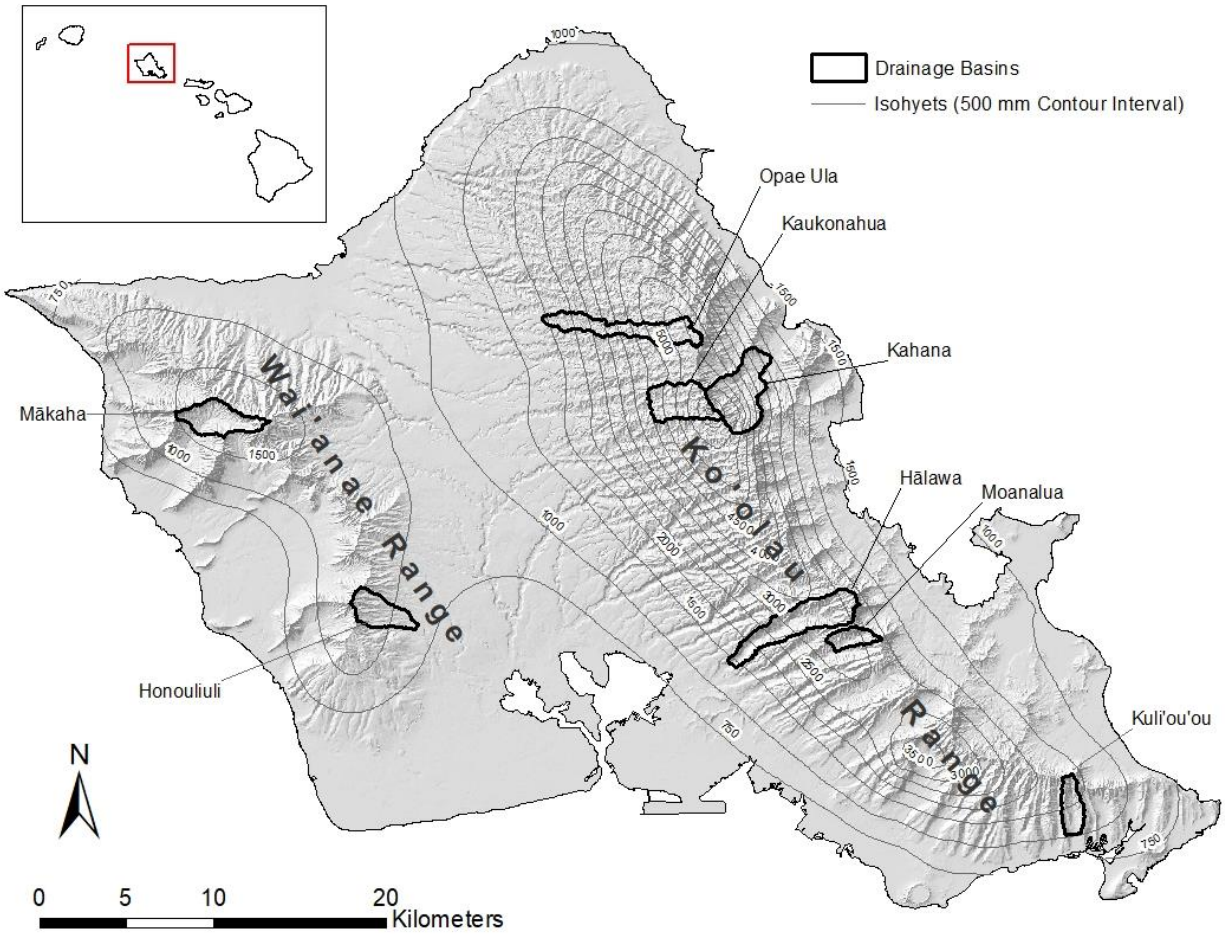

Figure 1. Digital elevation model (DEM) of the island of O‘ahu showing the location of the 8 drainage basins analyzed in this study outlined in black. Drainage basin selection was based on streamflow data continuity and overlap with high resolution gridded daily rainfall and temperature maps of Longman et al. (2019). Contour lines are mean annual isohyets from Giambelluca et al. (2013) for the 30-year period 1978-2007. The isohyet contour interval is 500 mm, and the isohyet range is 750 – 6500 mm. The Wai‘anae and Ko‘olau mountain ranges are labeled. UTM zone is 4N, and the projection is NAD 1983.

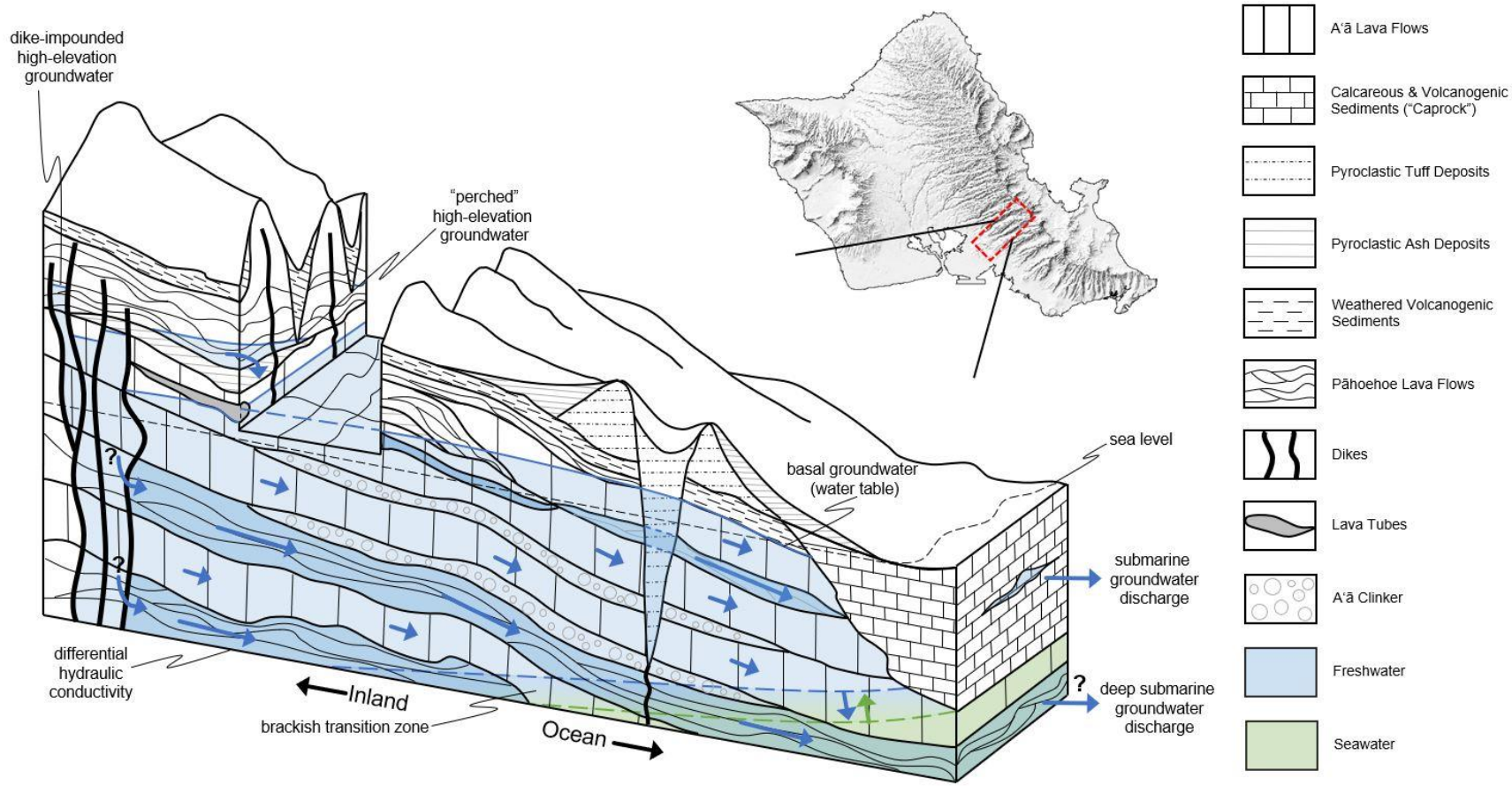

Figure 2. Cross section through a hypothetical slice of the leeward side of the Koʻolau Range on Oʻahu showing an inferred geohydrology. Figure not to scale. The length of arrows represents relative groundwater flow rate. Question marks indicate indirectly perceived aspects of the model.

1.3 Methodology Overview

Monthly recharge was estimated by creating a water budget model. A water budget is a tally of all the inputs to and outputs from a hydrologic system. The water budget model was tested in key areas of O‘ahu where it was possible to estimate each component of the water budget in at least two different ways, producing standard and experimental values for each. Before discussing the components of the water budget, it is necessary to define the hydrologic system, which in this case is a drainage basin, synonymous with the terms watershed and catchment (Ward & Trimble 2017). A drainage basin is a surface area that drains through a given point on the land surface. All land area falls within a drainage basin. Drainage basins do not overlap, and do not share surface water. While water residence times may vary, surface water that enters and travels across a drainage basin will eventually pass through the point by which the drainage basin is defined. The components of a water budget within a typical drainage basin include precipitation (P), evapotranspiration (ET), infiltration (I), changes in soil moisture storage (ΔSMS), changes in groundwater storage (ΔGWS), groundwater recharge (R), rapid surface flow (overland flow), and shallow subsurface flow (interflow) (Engott et al. 2015; Figure 3). Overland flow and interflow can be grouped together and are henceforth referred to as quickflow (QF) (Ward & Trimble 2017). In this study, the subsurface boundary of a drainage basin is assumed to be the boundary between the vadose and saturated zones (Figure 3). The overall water budget is simplified by assuming ΔSMS and ΔGWS are negligible. Recharge can then be estimated with only three parameters: P, ET, and QF (Expression 1).

$$P = I + ET + QF \pm \Delta SMS \pm \Delta GWS \quad (1a)$$

$$R = I \pm \Delta SMS \pm \Delta GWS \quad (1b)$$

$$\Delta SMS \pm \Delta GWS \approx 0 \quad (1c)$$

$$I \approx R \quad (1d)$$

$$P \approx R + ET + QF \quad (1e)$$

$$R \approx P - ET - QF \quad (1f)$$

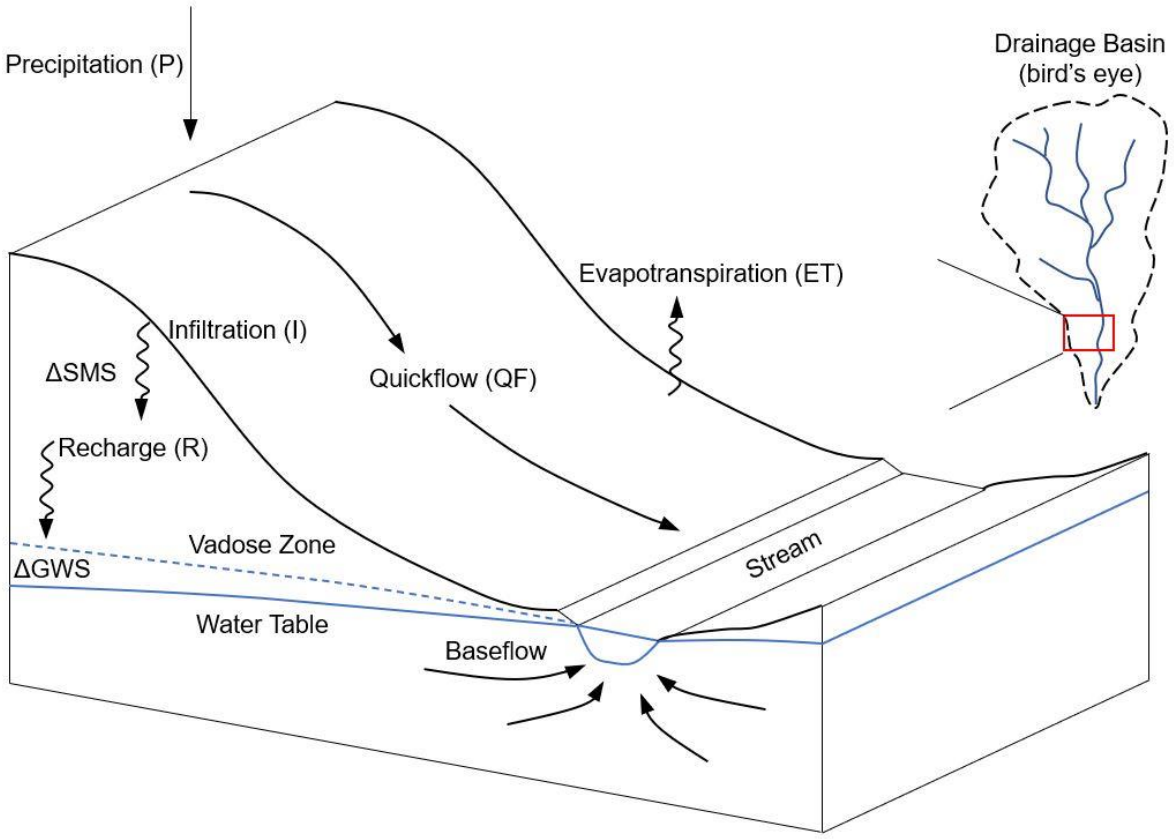

Figure 3. Cross section through a hypothetical drainage basin showing the components of a water budget. Figure not to scale, and modified from Figure 7-1, Dunne & Leopold (1978).

The first step in creating the water budget model in this study was to obtain monthly estimates of P, ET, and QF. High-resolution gridded climate mean and time-series data has become available over the last several years, which has vastly improved our understanding of climate trends throughout the state (Giambelluca et al. 2013; Frazier et al. 2016). Mean monthly rainfall maps that provide 30-year averaged monthly precipitation estimates for the entire state at 250m spatial resolution (Giambelluca et al. 2013) are available on the Rainfall Atlas of Hawai‘i at http://rainfall.geography.hawaii.edu/. Mean monthly evapotranspiration maps are also available (Giambelluca et al. 2014). These gridded datasets were interpolated from an extensive network of weather stations throughout the state, and have been meticulously curated, and widely applied in many Hawai‘i studies (Engott et al. 2015; Longman, Diaz & Giambelluca 2015; Wada et al. 2017; Krushelnycky et al. 2016; and others). Even more recently, daily gridded rainfall and temperature data have become available for the period from 1990-2014 (Longman et al. 2019). These daily precipitation and temperature maps are the foundation of the

water budget model developed in this study, and their application here is the major distinction between this water budget model and previous ones. The monthly precipitation values used in the model developed in this study were taken directly from the daily rainfall maps from Longman et al. (2019). Monthly ET values were derived from the daily temperature maps given in Longman et al. (2019). Monthly QF values were taken directly from information given by the United States Geological Survey (USGS) (Engott et al. 2015, Figure 7).

We tested the water budget model by determining uncertainty for each component of the model, and then propagating this error through the monthly recharge calculations to provide both a recharge range and multiple measures of agreement with a standard. We compared our calculated recharge values with the annual recharge estimates given by the USGS (Engott et al. 2015, Figure 10). Several factors make this USGS study an ideal standard for assessing the accuracy of the monthly water budget model developed in this study. First, the basic components of the USGS water budget developed by Engott et al. (2015) were generated using highly referenced datasets. Precipitation estimates were derived from the gridded rainfall data from Giambelluca et al. (2013) and then modified to match mean monthly precipitation from Giambelluca et al. (2013) (Engott et al. 2015, pp 16). Evapotranspiration estimates were taken from Giambelluca et al. (2014) (Engott et al. 2015, pp 27). Quickflow estimates for O‘ahu were derived from monthly precipitation maps (Frazier et al., 2016) and baseflow separations following Wahl & Wahl (1995) completed on 55 gauged streams across the Hawaiian Islands (Appendix A; Appendix B). These results were interpolated across ungauged drainage basins using regionally specific linear regressions (Engott et al. 2015, pp 20). Second, the USGS model accounts for many commonly neglected water budget components, like soil moisture storage, land cover variability, irrigation inputs, and septic-system leachate inputs (Engott et al. 2015). Finally, the USGS model differentiates between recharge during droughts and normal climate conditions, an important distinction that allows annual recharge to oscillate between two extremes depending on climate conditions (Engott et al., 2015). Together, these factors generate confidence in the accuracy of the USGS annual recharge estimates and justify using them as the standard for error analysis in this study.

2. Methods

2.1 Drainage Basin Selection

We selected eight drainage basins on Oʻahu to test the water budget calculations following the methodology described just above. Drainage basins were selected based on streamflow data availability, continuity, and overlap with the daily rainfall and temperature maps from Longman et al. (2019), which cover the period from 1/1/1990 to 12/30/2014. Streamflow data were obtained from the USGS National Water Information Service available at https://waterdata.usgs.gov/hi/nwis/sw. Twelve streams on Oʻahu had at least one year of continuous daily streamflow discharge measurements that overlapped with the daily rainfall and temperature maps. The field of available streams was further pared to eight by removing those with diversions upstream of the gauge, leaving Upper Kaukonahua, Kuliʻouʻou, Kahana, Opae Ula, Honouliuli, Moanalua, Mākaha, and Hālawa (Figure 1). It should be noted that Kahana and Mākaha are both known to be impacted by groundwater withdrawals (Engott et al. 2015; State of Hawaiʻi 2019) . These were retained for analysis based on our assumption that changes to groundwater storage would have a negligible impact on QF, ET, and infiltration processes, and based on the exclusion of ΔGWS from the simplified water balance (Expression 1).

2.2 Raster Analysis

The dimensions of each of the eight drainage basins were derived using the Environmental Systems Research Institute's (ESRI) proprietary Hydrology toolset in ArcMap. Daily rainfall maps were selected to match the available stream data periods, and then clipped to the drainage basin dimensions. This manipulation produced eight raster stacks of daily precipitation data - one raster stack for each drainage basin (Figure 4). Within each raster stack, each daily rainfall map was then averaged to provide a daily mean precipitation measurement for the entire drainage basin (Figure 4). The daily mean drainage basin precipitation values and the daily stream discharge values were then merged by date to produce eight data tables to be used as inputs for the monthly water budget calculations - one data table for each drainage basin (Figure 4). This same procedure was used to produce mean daily temperature estimates for each drainage basin from the daily temperature maps. These daily estimates were then aggregated to the monthly timescale to reduce processing time.

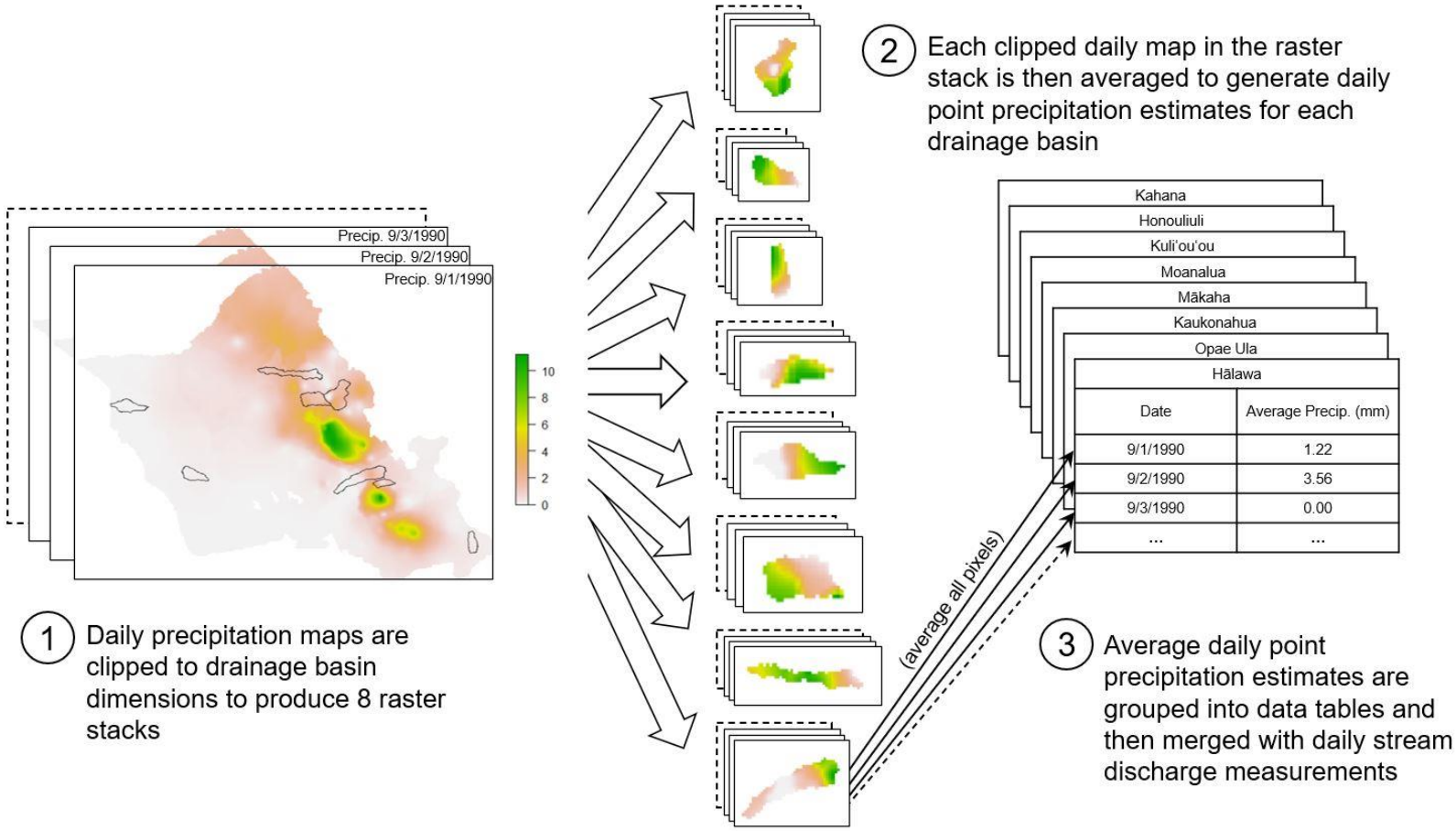

Figure 4. Conceptual depiction of the method used to generate daily average precipitation estimates from the daily rainfall maps in Longman et al. (2019).

2.3 Error Analysis

Uncertainty was propagated through the monthly water budget calculations to assess agreement with the USGS annual recharge estimates during both normal and drought-climate conditions. Quickflow uncertainty (δQF) was determined by taking the mean difference between the QF estimates in Engott et al. (2015, Figure 7) and estimates derived by completing stream hydrograph baseflow separations using daily streamflow measurements and the daily precipitation maps of Longman et al. (2019). Precipitation uncertainty (δP) was set as the median absolute deviation (MAD) from Longman et al. (2019, Table 3), which was 0.5 mm per pixel per day. Evapotranspiration uncertainty (δAET) was determined by taking the mean difference between the long-term average actual evapotranspiration (LTA-AET) maps of Giambelluca et al. (2014) and ET estimates derived using the Thornthwaite equation for potential evapotranspiration (PET). Monthly recharge uncertainty was determined by propagating each of these uncertainties through the monthly water budget calculations as follows:

$$\delta R = \left(\delta P^2 + \delta QF^2 + \delta ET^2\right)^{0.5} \tag{2}$$

In addition, three difference measures were calculated following Wilmott (1981, 1982a, 1982b) and Wilmott & Wicks (1980): Root mean square error (RMSE), mean absolute error (MAE), and index of agreement (d), calculated as follows:

$$RMSE = \left[N^{-1}\sum_{i=1}^{N}(S_i - E_i)^2\right]^{0.5} \tag{3}$$

$$MAE = N^{-1}\sum_{i=1}^{N}\left|S_i - E_i\right| \tag{4}$$

$$d = 1 - \left[\sum_{i=1}^{N}\left(S_i - E_i\right)^2 \Big/ \sum_{i=1}^{N}\left(|S_i'| + |E_i'|\right)^2\right] \tag{5}$$

, where N is the number of cases, E_i is the experimental output (predicted recharge), S_i is the standard output (USGS recharge), $S'_i = S_i - \bar{E}$, $\bar{E}$ is mean of the experimental output, $E'_i = E_i - \bar{E}$, and $0 \leq d \leq 1$. For the index of agreement, $d = 1$ indicates perfect agreement, and $d = 0$ indicates no agreement.

To complete the error analysis, it was necessary to disaggregate the USGS annual recharge estimates from Engott et al. (2015) down to the monthly timescale. This was done by applying a simple weighting factor to annual recharge for a particular drainage basin. Annual recharge was divided into 12 portions. Each monthly portion was then weighted by monthly precipitation according to the expression:

$$R_m = \frac{R_a}{12} \cdot \frac{P_m}{P_a} \tag{6}$$

, where R_m is monthly recharge, R_a is annual recharge, P_m is monthly precipitation, and P_a is annual precipitation. Monthly precipitation for each drainage basin was determined by aggregating the daily precipitation maps from Longman et al. (2019) to the monthly timescale. This adjustment maintains annual recharge totals from Engott et al. (2015) but allows monthly recharge to fluctuate with precipitation.

2.4 Quickflow

Monthly QF for each drainage basin was calculated directly from information given by Engott et al. (2015) who estimated QF on O‘ahu using one of two techniques depending upon the availability of streamflow data within a drainage basin. For the 16 drainage basins with a long enough continuous record of streamflow data, Engott et al. (2015) estimated QF by completing stream hydrograph baseflow separations following Wahl & Wahl (1995). For drainage basins without sufficient stream discharge data, Engott et al. (2015) estimated QF using regionally specific linear regressions based on statewide point precipitation and streamflow data (Engott et al. 2015, Table 5). The end results of this work are two maps that give QF ranges for each drainage basin on O‘ahu, one map for the dry season (May - October) and another for the wet season (November - April) (Engott et al. 2015, Figure 7). These ranges are given as runoff coefficients (RC), which are ratios of total QF to total precipitation. We took the mean of this RC range for each drainage basin to estimate monthly QF for the water budget model.

Quickflow uncertainty (δQF) was determined by taking the mean difference between a standard and an experimental value. The experimental QF in this study was the USGS seasonal QF estimates from Engott et al. (2015, Figure 7), previously mentioned. Standard QF was estimated using one of two procedures based on whether the stream within a drainage basin is ephemeral or perennial. For drainage basins with perennial streams, which included Upper Kaukonahua, Kuliʻouʻou, Kahana, Opae Ula, and Hālawa (Figure 1), we completed stream hydrograph baseflow separations to generate daily QF volumes for the period from 1/1/1990 - 12/31/2014 (Figure 5). The baseflow separations completed in this study differ from those completed by the USGS in that they are an average of two distinct baseflow separation techniques (Figure 5; Appendix A; Appendix B). The first baseflow separation technique used, hereafter referred to as the fixed five-day window (FFW) method, follows Wahl & Wahl (1995) and Engott et al. (2015) (Appendix A; Appendix B). The second technique follows Koskelo et al. (2012) and is known as the sliding average with rainfall record (SARR) method (Appendix A; Appendix B). The SARR baseflow separation method was selected because of its superior performance in capturing groundwater responses in small, flashy catchments in the mid-Atlantic region of the US (Koskelo et al. 2012). The results from these two techniques were averaged and aggregated to the monthly timescale. For ephemeral streams, which included Moanalua, Honouliuli, and Mākaha, no baseflow separation was necessary and all stream discharge was assumed to be QF. Despite excellent recent and on-going research, Mākaha stream's baseflow remains poorly quantified (Mair 2009, 2010; Shade 1984, Safeeq 2012; and others) so Mākaha was analyzed as both a perennial stream and an ephemeral stream. The monthly QF volumes derived from these two procedures were then compared with the experimental QF volumes from the USGS runoff maps of Engott et al. (2015, Figure 7). The mean difference between the two in each drainage basin was taken as the δQF.

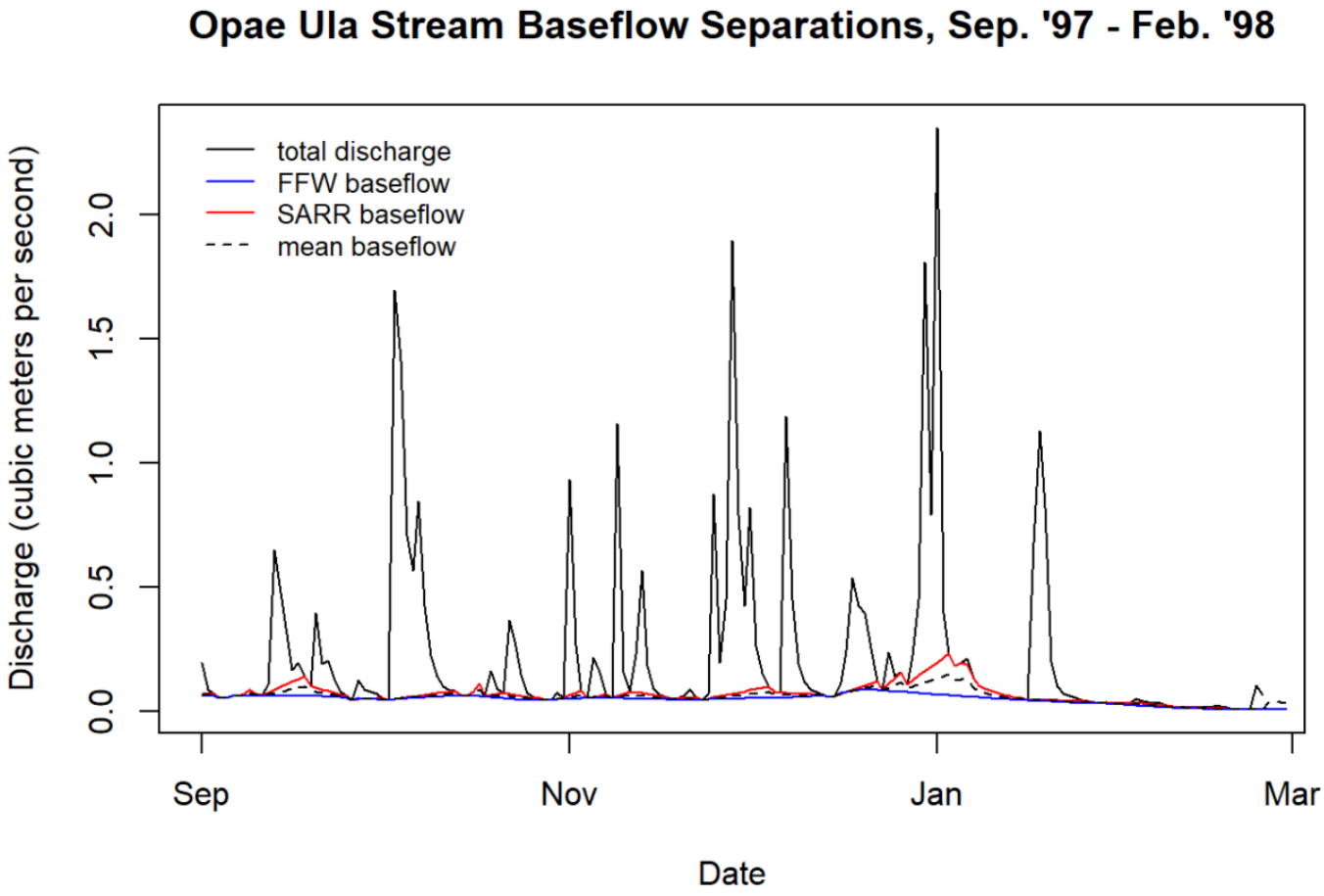

Figure 5. Stream hydrograph baseflow separation for Opae Ula stream for September 1997 – March 1998. Stream discharge data were obtained from the USGS National Water Information Service available at https://waterdata.usgs.gov/hi/nwis/sw. Two baseflow separation techniques are shown. Baseflow estimated using the fixed five-day window (FFW) technique following Wahl & Wahl (1995) is depicted in blue. Baseflow estimated using the sliding average with rainfall record (SARR) technique following Koskelo et al. (2012) is depicted in red. These two values were averaged and then used as an experimental value in error analysis.

2.5 Evapotranspiration

Monthly ET for each drainage basin was calculated using the Thornthwaite equation for potential evapotranspiration (PET), which has the advantage of only requiring mean monthly temperature as an input. The Thornthwaite PET is given by the expression:

$$PET_m = 1.6\left[\frac{10 \cdot T}{I}\right]^{\alpha} \tag{7a}$$

, where *m* is the specific month, *I* is the annual heat index, *T* is monthly mean temperature in degrees Celsius, and

$$\alpha = 0.49 + 1.79 \cdot 10^{-2} \cdot I - 7.71 \cdot 10^{-5} \cdot I^2 + 6.65 \cdot 10^{-7} \cdot I^3 \quad (7b)$$

The annual heat index (I) is given by:

$$I = \sum_{m=1}^{12} \left(\frac{T_m}{5} \right) \quad (7c)$$

The monthly temperature *(T)* and the annual heat index *(I)* were calculated for each drainage basin using the daily temperature maps from Longman et al. (2019) (Figure 4).

Potential evapotranspiration describes the maximum quantity of water that can be removed from the soil through evapotranspiration given a sufficient inventory of water. Actual evapotranspiration is the quantity of water that is actually removed from the soil after taking the available moisture into account. The Thornthwaite PET (Expression 2) was converted to AET in this study by limiting PET to the moisture available from precipitation, ignoring soil moisture for simplicity. The quantity of precipitation available for AET was derived directly from the daily rainfall maps in Longman et al. (2019). This technique is henceforth referred to as the precipitation-limited Thornthwaite actual evapotranspiration (PLT-AET)

The Thornthwaite PET is not the preferred method for estimating PET so the decision to use it in this study had to be validated with empirical data (Dunne & Leopold 1978). The preferred method for estimating PET uses an equation developed by Penman (1948) and Monteith (1965) and is referred to as the Penman-Monteith equation for PET (Montieth 1965; Giambelluca et al., 2014; Engott et al., 2015; Dunne & Leopold 1978). Several forms of the Penman-Monteith equation exist. The one used in this study follows the American Society of Civil Engineers (Allen et al., 2005), and is given by the expression:

$$PET_{PM} = \frac{0.408\Delta(R_n - G) + \gamma \frac{C_n}{T+273} u_2 (e_s - e_a)}{\Delta + \gamma(1 + C_d u_2)} \quad (8)$$

, where:

PET_{PM} is the reference evapotranspiration for short surfaces given in mm d^{-1},

R_n is calculated net radiation at the crop surface given in MJ m^{-2} d^{-1},

G is soil heat flux density at the soil surface given in MJ m^{-2} d^{-1},

T is mean daily temperature at 1.5 to 2.5-m height (°C),

u_2 is mean daily wind speed at 2-m height given in m s^{-1},

e_s is saturation vapor pressure at 1.5 to 2.5-m height (kPa),

e_a is mean actual vapor pressure at 1.5 to 2.5-m height (kPa),

Δ is the slope of the saturation vapor pressure-temperature curve given in kPa $°C^{-1}$,

γ is the psychrometric constant given in kPa $°C^{-1}$,

C_n is a numerator constant that changes with crop reference type and calculation time step, and

C_d is the denominator constant that changes with reference type and calculation time step.

The Penman-Montieth formula is an energy-balance which expresses the net energy accumulation at the soil surface as a measurement of PET. The amount of moisture this accumulated energy can remove from soil depends on vegetation, soil characteristics and available moisture. These physical characteristics are captured in a parameter called the crop coefficient (K_c), which varies by land cover, and can be multiplied by the Penman-Monteith PET to convert to AET (Montieth 1965; Allen et al. 2005).

To assess the accuracy of the PLT-AET method and to determine δAET for the water budget model error analysis, we completed an additional ET micro-study using atmospheric data from a weather station in Pearl City, HI. In this micro-study we compared the PLT-AET method with the LTA-AET maps from Giambelluca et al. (2014), which were used to estimate annual recharge in the USGS study (Engott et al. 2015). Our goal was to determine which method (the PLT-AET or the LTA-AET maps) did a better job predicting AET at the weather station. We used the Penman-Monteith equation to calculate the standard AET at the weather station. We then assessed the agreement between the experimental values and the standard using the difference measures previously mentioned (Expressions 3-5). The stronger of the two experimental values was used to determine monthly AET, and the mean difference between two was set as δAET for the water budget model error analysis.

The Pearl City weather station dataset covered the period from December 2019 to December 2020, and included measurements of temperature, humidity, precipitation, windspeed, and solar radiation. These data were collected using an OnSet Computer Corporation© (Bourne, Massachusetts) portable weather station mounted on a 3-meter M-TPA-KIT portable tripod, equipped with the OnSet Computer Corporation© HOBO series of sensors, and powered by a 5-watt solar panel and 12 volt storage battery. Data were averaged over 15-minute intervals using a HOBO RX3000 Remote Monitoring Station running HOBOware Pro 3.7.22 software. Rain was measured with a HOBO 2-RGx-M002 tip bucket rain gauge that has a 15.4 cm receiving orifice and measures rainfall rates up to 20 mm/hour. Solar radiation was measured with HOBO S-LIB-M003 silicon pyranometer with a measurement range of 0 to 1280 W/m2. Temperature and relative humidity were measured with a HOBO S-THB-M00X Temperature/Relative Humidity Sensor with a temperature range of -40 to 75 ˚C and an accuracy of +/- 0.2 ˚C. The relative humidity range was from 0 to 100 percent with an accuracy of ± 2.5 percent. Atmospheric pressure was measured using a HOBO S-BPB-CM50 Barometric Pressure Sensor with a range from 660 to 1070 millibar and an accuracy of ±3 millibar. Wind speed was measured with a HOBO S-WSET-B wind speed/wind director sensor set. This sensor set had a range from 0 to 76 m/s with an accuracy of +/- 1.1 m/s or 4 percent of the sensor output, whichever is greater. Net radiation was calculated from solar radiation measurements using Equations 15, 16, 18, and 20 of Allen et al. (2005). Clear sky radiation was computed using the model of Bird and Hulstrom (1981). The climate monitoring station was in an area of cropped grass at 21.417299 N and -157.948142 W at an elevation of 154 m above mean sea level, with a K_c value of 1. Measured wind speed was corrected to a 2 m height using Equation 33 of Allen et al. (2005).

2.6 Fog Drip

Fog drip was accounted for in each drainage basin prior to estimating recharge. Fog estimates were obtained from Engott et al. (2015), who provided monthly fog estimates as ratios of fog drip to rainfall following Ekern (1983) and Engott & Vana (2007). These monthly fog estimates were normalized and then applied to the total annual fog drip from Engott et al. (2015) to provide monthly fog drip volumes for each drainage basin. These monthly fog drip volumes were added to precipitation totals in the water budgets.

3. Results & Interpretation

3.1 Overview

The recharge estimates generated using the method presented here showed strong agreement with the annual long-term averages given by the USGS. Average monthly experimental recharge behaved as expected through most drainage basins, with higher recharge generally occurring during the wet season and lower recharge during the dry season (Tables 1 & 2). Monthly experimental recharge peaked in March for most drainage basins and reached a low between July and September (Table 1 & 2). Several drainage basins showed a small spike in recharge during the month of July, which may be related to high historical consistency in the Northeast Trade Winds during this period each year (Table 1 & 2). Mean annual experimental recharge varied from 1.93 Mm^3y^{-1} in Kuli‘ou‘ou to 16.87 Mm^3y^{-1} in Hālawa (Table 3). Experimental recharge uncertainty (δR) was relatively high compared to total mean annual experimental recharge for several drainage basins, most notably in Kuli‘ou‘ou and Honouliuli, where δR was approximately 94% and 93% of total mean annual experimental recharge, respectively (Table 3; Figure 6). After correcting for an apparent anomaly in the Kuli‘ou‘ou drainage basin, agreements ranged from 0.62 in the Honouliuli drainage basin, indicating moderate agreement, to 0.96 in the Opae Ula drainage basin, indicating very strong agreement (Table 3; Figures 6 & 7). Interannual trends in experimental recharge matched periods of historical drought identified by Frazier et al. (*in review*; Figures 6 & 7). There were also notable departures from long-term average standard recharge in the Kahana and Mākaha drainage basins. The USGS long-term average recharge in Kahana is 26 Mm^3y^{-1} during normal climate conditions and 20 Mm^3y^{-1} during drought conditions. Mean annual experimental recharge was substantially lower (16 Mm^3y^{-1}; Table 3). The data show the opposite trend in Mākaha. Mean annual experimental recharge exceeded USGS long-term average recharge by 2.0 x 10^5 m^3y^{-1} (Table 3). Agreements for both Kahana and Mākaha remained relatively high, 0.82 and 0.72 respectively, likely due to the high experimental recharge uncertainty in both drainage basins (Table 3).

Table 1. Monthly water budgets for Kaukonahua, Hālawa, Opae Ula and Kahana drainage basins on the island of Oʻahu. Drainage basins were selected for continuity and overlap with the daily rainfall maps in Longman et al. (2019). Abbreviations: P is precipitation; PLT-AET is precipitation-limited Thornthwaite actual evapotranspiration; QF is quickflow; Obs. QF is observed QF derived from either stream discharge measurements or completing stream hydrograph baseflow separations; R is recharge. All units are in million cubic meters per year ($Mm^3\ y^{-1}$).

		Jan	Feb	Mar	Apr	May	June	July	Aug	Sep	Oct	Nov	Dec	Ann
Kaukonahua	P	2.429	2.508	3.413	2.579	2.304	2.008	2.197	2.219	2.531	2.943	3.162	2.813	31.108
	PLT-AET	0.410	0.389	0.380	0.439	0.439	0.469	0.484	0.520	0.555	0.516	0.470	0.406	5.476
	QF	0.911	0.941	1.280	0.967	0.864	0.753	0.824	0.832	0.949	1.104	1.186	1.055	11.665
	BFS QF	0.590	0.533	0.815	0.674	0.575	0.555	0.734	0.590	0.632	0.639	0.871	0.731	7.939
	R	1.220	1.262	1.797	1.217	1.012	0.853	0.939	0.899	1.055	1.329	1.535	1.413	14.532
Hālawa	P	2.473	2.012	3.166	2.228	1.957	2.003	2.428	1.848	2.153	2.607	3.103	2.814	28.791
	PLT-AET	0.589	0.601	0.621	0.642	0.538	0.629	0.714	0.593	0.691	0.782	0.779	0.630	7.811
	QF	0.495	0.402	0.633	0.446	0.196	0.200	0.243	0.185	0.215	0.261	0.621	0.563	4.459
	BFS QF	0.421	0.269	0.619	0.273	0.237	0.124	0.188	0.157	0.152	0.248	0.501	0.471	3.660
	R	1.457	1.059	1.938	1.167	1.230	1.215	1.502	1.089	1.264	1.567	1.721	1.658	16.867
Opae Ula	P	2.256	2.153	2.976	2.282	2.095	1.878	2.079	1.832	1.950	2.388	2.746	2.545	27.180
	PLT-AET	0.441	0.451	0.447	0.501	0.474	0.523	0.540	0.517	0.538	0.590	0.552	0.461	6.036
	QF	0.846	0.808	1.116	0.856	0.419	0.376	0.416	0.366	0.390	0.478	1.030	0.954	8.054
	BFS QF	0.896	0.707	1.244	0.655	0.615	0.358	0.483	0.422	0.411	0.690	1.087	0.823	8.392
	R	1.198	1.067	1.505	1.017	1.224	1.117	1.226	1.018	1.079	1.331	1.221	1.256	14.260
Kahana	P	3.134	2.497	3.604	2.676	2.855	2.083	2.206	2.522	2.332	2.917	3.252	2.890	32.970
	PLT-AET	0.634	0.556	0.567	0.629	0.580	0.620	0.625	0.706	0.696	0.731	0.705	0.587	7.635
	QF	0.627	0.499	0.721	0.535	0.571	0.417	0.827	0.946	0.875	1.094	1.220	1.084	9.415
	BFS QF	1.231	1.126	1.943	0.939	1.410	0.368	0.650	0.561	0.694	0.990	1.481	1.176	12.569
	R	1.884	1.453	2.328	1.522	1.716	1.058	0.765	0.881	0.773	1.103	1.339	1.230	16.052

Table 2. Monthly water budgets for Mākaha Moanalua, Kuliʻouʻou, and Honouliuli drainage basins on the island of Oʻahu. Drainage basins were selected for continuity and overlap with the daily rainfall maps in Longman et al. (2019). Abbreviations: P is precipitation; PLT-AET is precipitation-limited Thornthwaite actual evapotranspiration; QF is quickflow; Obs. QF is observed QF derived from either stream discharge measurements or completing stream hydrograph baseflow separations; R is recharge. All units are in million cubic meters per year ($Mm^3\ y^{-1}$).

		Jan	Feb	Mar	Apr	May	June	July	Aug	Sep	Oct	Nov	Dec	Ann
Mākaha	P	1.041	0.669	1.025	0.518	0.603	0.303	0.225	0.270	0.329	0.567	0.839	1.200	7.587
	PLT-AET	0.257	0.216	0.259	0.173	0.184	0.101	0.072	0.087	0.110	0.183	0.252	0.256	2.149
	QF	0.036	0.023	0.036	0.018	0.021	0.011	0.022	0.027	0.033	0.057	0.084	0.120	0.488
	BFS QF	0.105	0.075	0.140	0.035	0.026	0.004	0.002	0.001	0.001	0.007	0.028	0.116	0.540
	R	0.753	0.461	0.754	0.343	0.410	0.194	0.143	0.185	0.239	0.368	0.524	0.845	5.219
Moanalua	P	0.601	0.664	1.317	0.677	0.649	0.558	0.766	0.397	0.479	0.728	0.637	0.583	8.056
	PLT-AET	0.168	0.178	0.174	0.180	0.199	0.182	0.185	0.127	0.158	0.188	0.167	0.158	2.065
	QF	0.060	0.066	0.132	0.067	0.064	0.055	0.076	0.039	0.048	0.073	0.063	0.058	0.800
	Disch.	0.026	0.079	0.384	0.105	0.083	0.015	0.223	0.053	0.005	0.104	0.106	0.048	1.230
	R	0.374	0.420	1.011	0.430	0.385	0.321	0.505	0.231	0.273	0.467	0.406	0.367	5.191
Kuliʻouʻou	P	0.465	0.388	0.185	0.148	0.138	0.058	0.161	0.251	0.200	0.341	0.390	0.397	3.122
	PLT-AET	0.150	0.139	0.060	0.049	0.045	0.019	0.052	0.081	0.067	0.110	0.130	0.128	1.029
	QF	0.016	0.014	0.006	0.015	0.014	0.006	0.016	0.025	0.020	0.012	0.014	0.014	0.171
	BFS QF	0.006	0.003	0.006	0.006	0.003	0.002	0.005	0.030	0.004	0.018	0.070	0.031	0.185
	R	0.300	0.237	0.119	0.085	0.081	0.035	0.095	0.146	0.114	0.219	0.247	0.256	1.934
Honouliuli	P	0.699	0.252	0.474	0.313	0.911	0.198	0.231	0.110	0.283	0.453	0.152	0.320	4.395
	PLT-AET	0.225	0.087	0.151	0.103	0.293	0.066	0.073	0.033	0.089	0.142	0.048	0.101	1.409
	QF	0.024	0.008	0.016	0.011	0.032	0.007	0.023	0.010	0.027	0.044	0.014	0.031	0.248
	Disch.	0.009	0.004	0.001	0.001	0.006	0.000	0.003	0.000	0.004	0.016	0.001	0.009	0.052
	R	0.450	0.157	0.307	0.200	0.587	0.125	0.135	0.067	0.168	0.266	0.089	0.188	2.739

Table 3. Error propagation through monthly water budget calculations for eight drainage basins on the island of Oʻahu. Abbreviations: P is precipitation; δP is precipitation uncertainty; PLT-AET is precipitation-limited Thornthwaite actual evapotranspiration; δAET is actual evapotranspiration uncertainty; QF is quickflow; Obs. QF is observed QF estimates derived from either stream discharge measurements or stream hydrograph baseflow separations following Wahl & Wahl (1995) and Koskelo et al. (2012); R is recharge; δR is recharge uncertainty; USGS is United States Geological Survey; NC is normal climate; DC is drought climate; RMSE is root mean square error; MAE is mean absolute error. δP, δAET, δQF, and δR all describe annual uncertainty. RMSE, MAE and agreement were calculated following Wilmott (1981, 1982a, 1982b) and Wilmott & Wicks (1980), and reflect the variability in monthly recharge estimates compared to the recharge predictions given by the USGS (Engott et al., 2015).

	Units	Kaukonahua	Hālawa	Opae Ula	Kahana	Mākaha	Moanalua	Kuliʻouʻou	Honouliuli
Area	Mm^2	6.59	10.37	7.81	9.67	5.93	2.39	3.30	4.86
P	Mm^3	31.11	28.79	27.18	32.97	7.59	8.06	3.12	4.39
δP	$mm\ d^{-1}$	0.50	0.50	0.50	0.50	0.50	0.50	0.50	0.50
δP	Mm^3	1.20	1.89	1.43	1.76	1.08	0.44	0.60	0.89
PLT-AET	Mm^3	5.48	7.81	6.04	7.64	2.15	2.06	1.03	1.41
LTA-AET	Mm^3	5.64	9.27	7.17	8.86	5.53	2.17	2.72	3.81
δAET	Mm^3	0.17	1.46	1.14	1.23	3.38	0.10	1.69	2.40
QF	Mm^3	11.67	4.46	8.05	9.42	0.49	0.80	0.17	0.25
Obs. QF	Mm^3	7.94	3.66	8.39	12.57	0.54	2.46	0.37	0.10
δQF	Mm^3	3.73	0.80	0.34	3.15	0.05	1.66	0.20	0.14
R	Mm^3	14.53	16.87	14.26	16.05	5.22	5.19	1.93	2.74
δR	Mm^3	3.92	2.52	1.86	3.82	3.55	1.72	1.81	2.56
R USGS NC	Mm^3	15.37	16.68	14.16	25.68	5.03	3.94	1.57	1.42
R USGS DC	Mm^3	12.10	13.46	10.23	19.51	2.19	2.73	0.51	0.40
RMSE	$10^4\ m^3$	39.98	61.31	31.21	102.82	37.89	11.20	11.93	13.19
MAE	$10^4\ m^3$	25.48	41.53	23.04	66.65	19.23	8.04	10.28	10.64
Agreement	DN	0.92	0.83	0.96	0.82	0.72	0.79	0.17	0.62

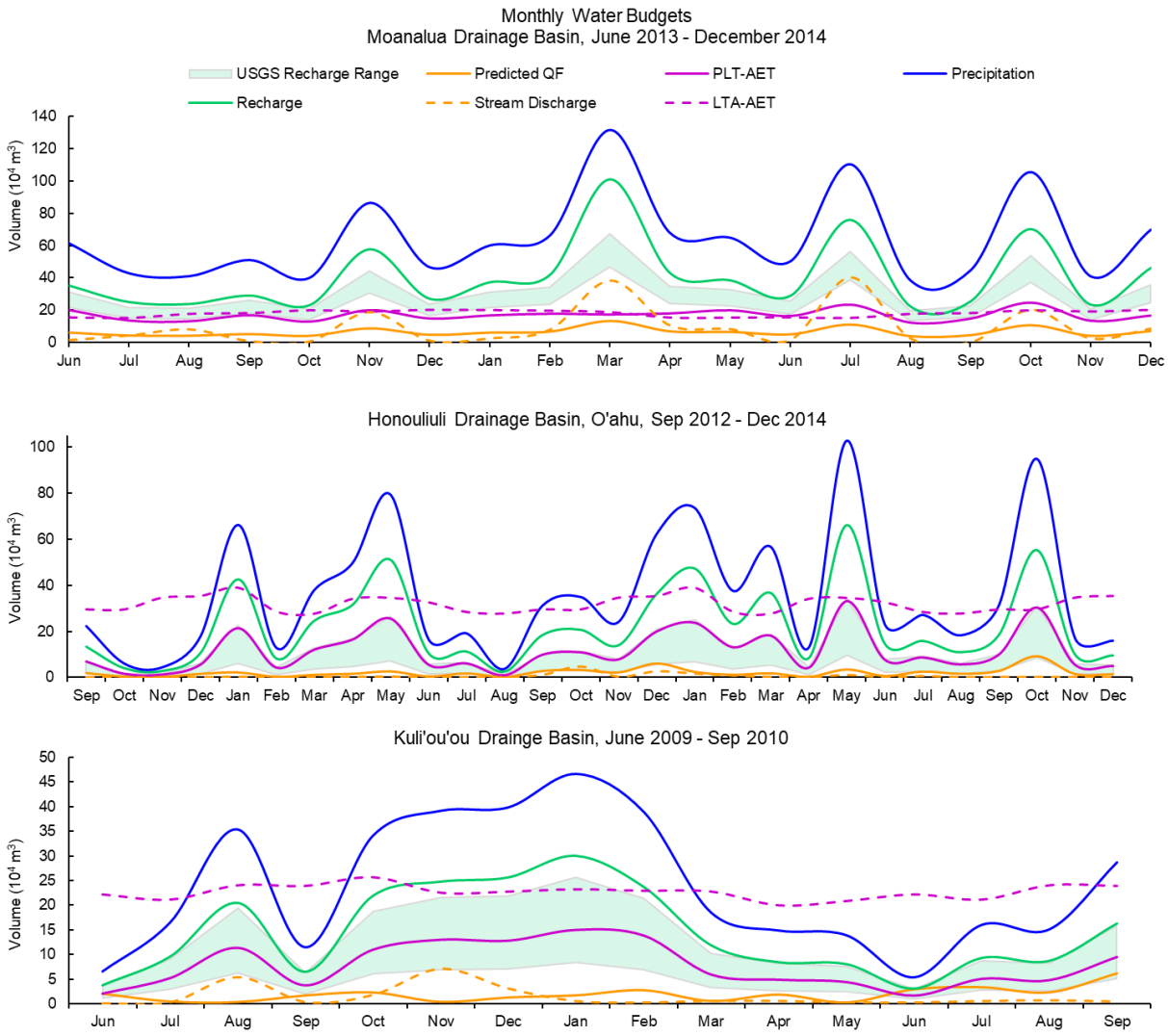

Figure 6. Monthly water budgets derived from daily gridded precipitation data (Longman et al. 2019) for the Moanalua **(7A)**, Kuli‘ou‘ou **(7C)**, and Honouliuli **(7B)** drainage basins on the island of O‘ahu. USGS recharge was disaggregated to monthly timescale by volume-weighting according to monthly precipitation. Recharge estimates are taken from Engott et al. (2015). **(7A)** Annual recharge for the Moanalua drainage basin was 5.2 ± 0.6 $Mm^3\ y^{-1}$. USGS annual recharge is 3.9 $Mm^3\ y^{-1}$ during normal climate conditions, and 2.7 $Mm^3\ y^{-1}$ during drought conditions. **(7B)** Annual recharge for the Honouliuli drainage basin was 2.7 ± 2.6 $Mm^3\ y^{-1}$. USGS annual recharge is 1.4 $Mm^3\ y^{-1}$ during normal climate conditions, and 0.5 $Mm^3\ y^{-1}$ during drought conditions. **(7C)** Annual recharge for the Kuli‘ou‘ou drainage basin was 1.9 ± 1.8 $Mm^3\ y^{-1}$. USGS annual recharge is 1.6 $Mm^3\ y^{-1}$ during normal climate conditions, and 0.5 $Mm^3\ y^{-1}$ during drought conditions.

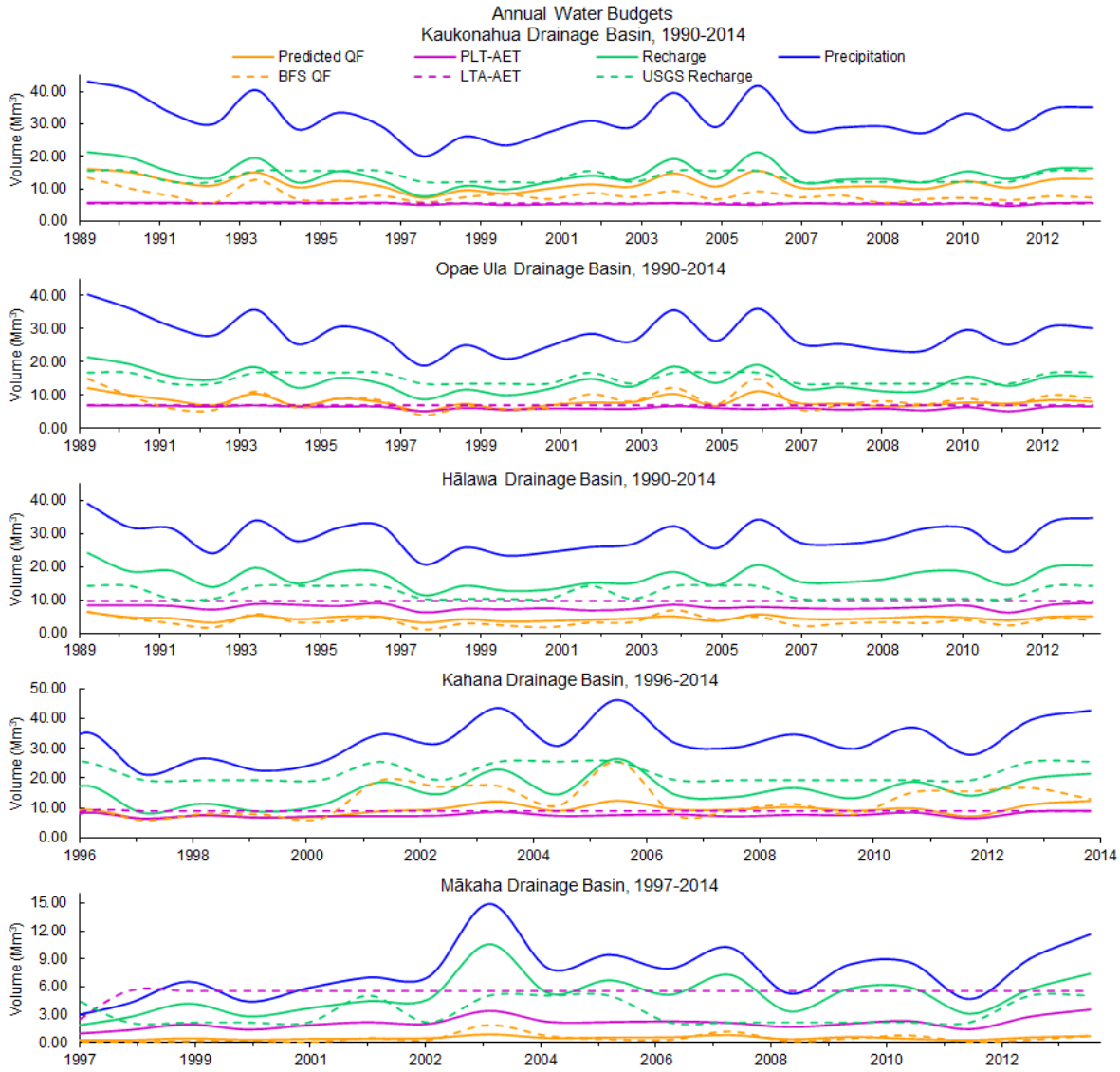

Figure 7. Annual water budgets derived from daily gridded precipitation and temperature data (Longman et al. 2019) for Kaukonahua **(6A)**, Opae Ula **(6B)**, Hālawa **(6C)**, Kahana **(6D)**, and Mākaha **(6E)** drainage basins on the island of Oʻahu. USGS recharge estimates are derived from Engott et al. (2015) and oscillate between drought and normal climate conditions. **(6A)** Mean annual recharge for the Kaukonahua drainage basin was 14.5 ± 3.9 Mm3 y^{-1}. USGS annual recharge is 15.4 Mm^3 during normal climate conditions, and 12.1 Mm^3 during drought conditions. **(6B)** Mean annual recharge for the Opae Ula drainage basin was 14.3 ± 1.9 Mm3 y^{-1}. USGS annual recharge is 16.7 Mm3 during normal climate conditions, and 13.5 Mm3 during drought conditions. **(6C)** Mean annual recharge for the Hālawa drainage basin was 16.9 ± 2.5 Mm^3 y^{-1}. USGS annual recharge is 14.2 Mm^3 y^{-1} during normal climate conditions, and 10.2 Mm^3 y^{-1} during drought conditions. **(6D)** Mean annual recharge for the Kahana drainage basin was 16.1 ± 3.8 Mm^3 y^{-1}. USGS annual recharge is 25.7 Mm^3 y^{-1} during normal climate conditions, and 19.5 Mm^3 y^{-1} during drought conditions. **(6E)** Mean annual recharge for the Mākaha drainage basin was 5.2 ± 3.5 Mm^3 y^{-1}. Estimated annual recharge is 5.0 Mm^3 y^{-1} during normal climate conditions, and 2.2 Mm^3 y^{-1} during drought conditions.

3.2 Quickflow Error

Temporal resolution and uncertainty play important roles in assessing the agreement between observed QF and the standard. At the seasonal timescale, both the SARR and FFW baseflow separations performed well, producing strong agreement with the runoff coefficients from Engott et al. (2015). In contrast, monthly observed QF estimates were poorly constrained, fluctuating more widely about seasonal means than expected, particularly for Kahana and Mākaha where more than 70% of monthly estimates exceeded the RC ranges in Engott et al. (2015) (Figure 8). Throughout all drainage basins, no more than 48% of monthly QF estimates fell within the RC ranges from Engott et al. (2015). These discrepancies produced large uncertainties in drainage basins with high QF (Table 2). It is likely that systematic differences between the long-term average precipitation maps from Giambelluca et al. (2013) and the daily rainfall maps from Longman et al. (2019) contributed to this large uncertainty (Figure 9). These systematic differences could be the result of a long-term shift in precipitation trends throughout the state, or they could simply indicate that the long-term average data are not a good representation of the period examined. It is also possible that the baseflow separations simply produced poor results for some drainage basins. Since a baseflow separation is a graphical as opposed to empirical procedure (the latter such as a chemical baseflow separation), it is impossible to truly assess its accuracy. Overall, these results generate confidence that the RC ranges from Engott et al. (2015) are useful for estimating seasonal QF. They also show that downscaling to the monthly timescale produces high uncertainty, and they emphasize the hazard of applying long-term averages to time-series data. Additionally, the strong agreement between seasonal QF estimates derived from the SARR baseflow separation and the USGS runoff coefficients suggests that the SARR method is a valid technique for differentiating baseflow from QF in gauged Hawaiian streams.

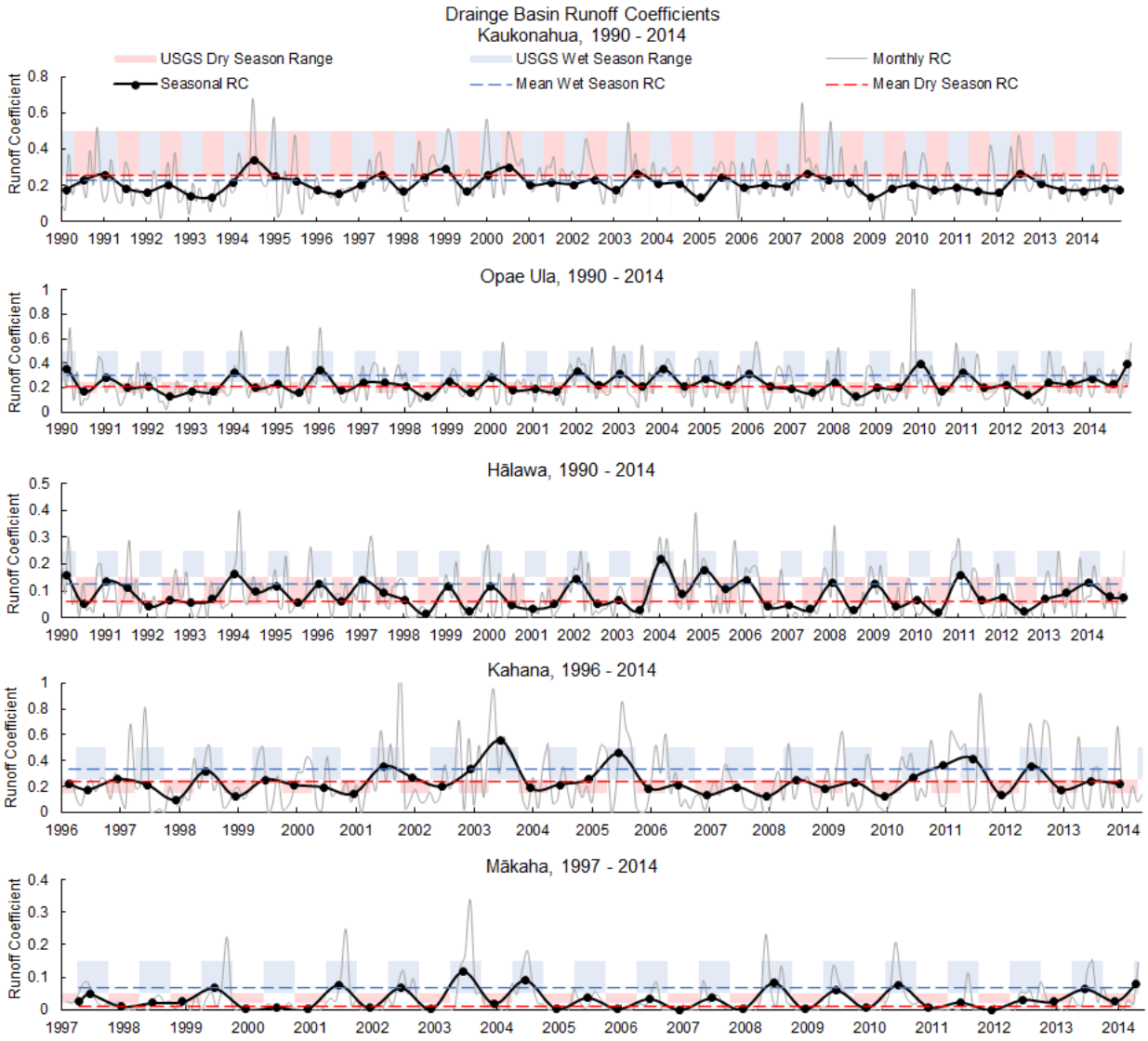

Figure 8. Runoff coefficients (RC) derived from stream hydrograph baseflow separations for five drainage basins on O‘ahu compared with seasonal RC ranges given by the USGS (Engott et al., 2015, Figure 7). Baseflow separations were carried out following Wahl & Wahl (1995) and Koskelo et al. (2012) and averaged. Stream discharge data were obtained from the USGS National Water Information Service available at https://waterdata.usgs.gov/hi/nwis/sw. **(8A)**: The USGS RC range for Kaukonahua was 0.25 - 0.50 through the wet and dry seasons. The mean wet season RC was 0.23. The mean dry season RC was 0.26. **(8B)**: The USGS RC range for Opae Ula was 0.25 - 0.50 through the wet season and 0.15 - 0.25 through the dry season. The mean wet season RC was 0.30. The mean dry season RC was 0.21. **(8C)**: The USGS RC range for Hālawa was 0.15 - 0.25 through the wet season and 0.05 - 0.15 through the dry season. The mean wet season RC was 0.12. The mean dry season RC was 0.06. **(8D)**: The USGS RC range for Kahana was 0.25 - 0.50 through the wet season and 0.15 - 0.25 through the dry season. The mean wet season RC was 0.34. The mean dry season RC was 0.24. **(8E)**: The USGS RC range for Mākaha was 0.05 - 0.15 through the wet season and 0.02 - 0.05 through the dry season. The mean wet season RC was 0.07. The mean dry season RC was 0.01.

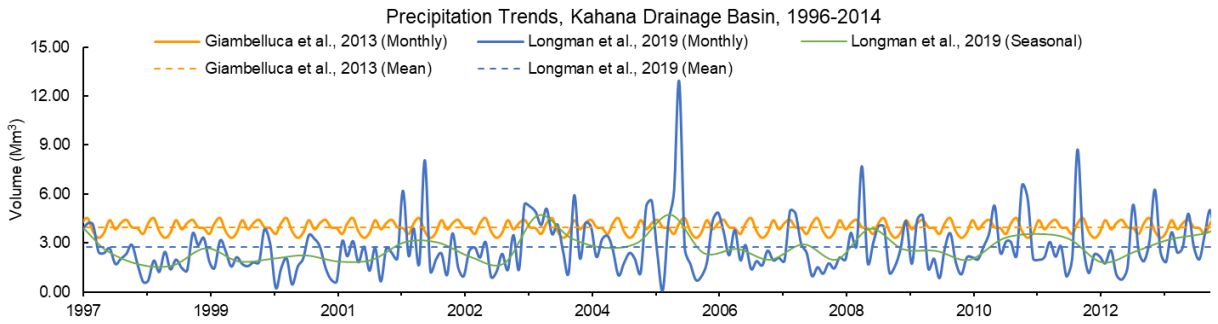

Figure 9. Precipitation trends for the Kahana drainage basin. The orange lines depict 30-year average monthly precipitation estimates taken from Giambelluca et al. (2013) and reflect average precipitation for the Kahana drainage basin from 1978 - 2007. The blue and green lines depict monthly, seasonal, and mean precipitation estimates derived from daily rainfall maps of Longman et al. (2019). Mean precipitation from Giambelluca et al. (2013) is 47.5 Mm^3 y^{-1}. Mean precipitation from Longman et al., (2019) is 33.1 Mm^3 y^{-1}.

3.3 Evapotranspiration Error

When compared with the LTA-AET estimates from Giambelluca et al. (2014), the PLT-AET estimates show stronger agreement with the weather station AET data from Pearl City, HI (Figure 10). The PLT-AET model produced an agreement of 0.60 with the weather station data, whereas the LTA-AET estimates produce an agreement of 0.40. RMSE and MAE were 29.4 and 23.1 mm per month, respectively, for the PLT-AET method, and 31.5 and 25.7 mm per month, respectively, for the LTA-AET estimates. The total annual standard AET calculated using the Penman-Monteith equation (Expression 3) is 756 mm, the total annual PLT-AET calculated using Expression 2 is 746 mm, and the total annual LTA-AET was 948 mm. The large gap separating the LTA-AET from the Penman-Monteith AET and PLT-AET is due primarily to differences during the dry season, which suggests a systematic offset (Figure 10). In contrast, for most months the Penman-Monteith AET and the PLT-AET are within 15 mm. The largest gaps between these occur during the months of April and October and are likely a consequence of excluding soil moisture storage from the PLT-AET calculations. In April, the Penman-Monteith AET exceeds the PLT-AET by approximately 40 mm. In October the opposite occurs: PLT-AET exceeds the Penman-Monteith AET by more than 70 mm. These offsets correspond to the seasonal changes one would expect in soil moisture content. High soil moisture at the end of the wet season would increase the total volume of moisture available for ET, thus increasing the PLT-AET. Low soil moisture at the end of the dry season would reduce the total moisture

available for ET, thus decreasing PLT-AET. It is possible, therefore, that future iterations of the PLT-AET model could be improved by a simple correction related to seasonal changes in soil moisture storage.

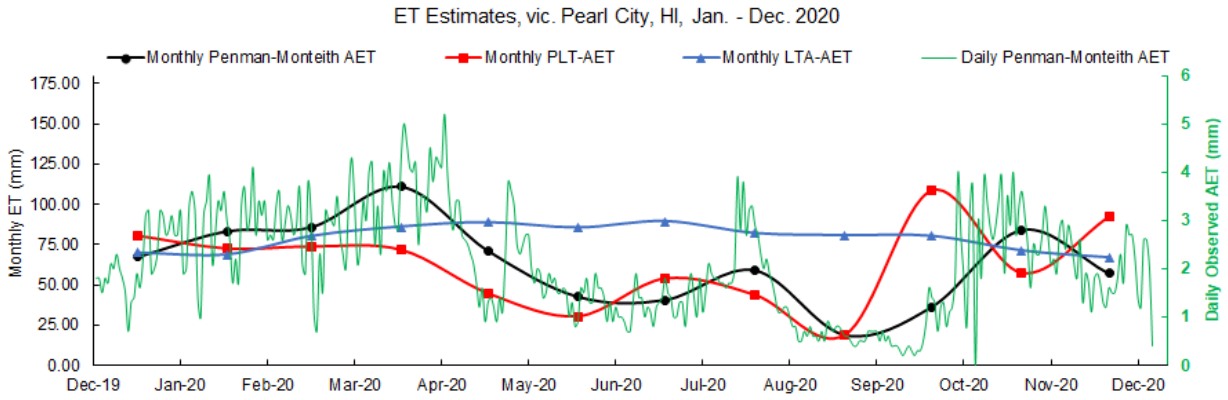

Figure 10. Actual Evapotranspiration (AET) estimates for a weather station in the vicinity of Pearl City, HI from Jan. to Dec. 2020 derived using the Penman-Monteith formula compared with precipitation-limited (PL) potential evapotranspiration (PET) and long-term average (LTA) AET. LTA-AET was taken from the monthly rainfall maps in Giambelluca et al. (2014). The PL-PET estimates were derived using the daily temperature maps from Longman et al. (2019) as inputs to the Thornthwaite equation for monthly PET. Daily AET at the weather station is shown in green along the right vertical axis.

The differences between the PLT-AET and Penman-Monteith AET likely stem from not considering soil moisture storage in the PLT-AET model. Soil moisture storage can constitute a large portion of the total moisture available for ET in some areas (Engott et al., 2015). Since the LTA-AET estimates consider soil moisture, it is possible that these are more accurate in some cases. The Pearl City field site data show that the LTA-AET estimates are marginally closer to the Penman-Monteith AET during 4 out of 12 months (Figure 10), which partially justifies this conclusion. These errors were propagated through the water budget calculations by setting δAET as the mean difference between the LTA-AET and PLT-AET estimates. This procedure was necessary to accurately capture the uncertainty in the PLT-AET estimates, but it produced the highest error of all the water budget components (Table 3). Overall, the results from the ET micro-study justified the application of the PLT-AET technique to the eight drainage basins and allowed the generation of monthly AET estimates across the entire study period utilizing the daily temperature and precipitation maps of Longman et al. (2019).

3.4 Recharge Error

Monthly recharge estimates derived from the daily gridded rainfall and temperature maps generally showed strong agreement with USGS recharge estimates (Table 3, Figures 6 & 7), and seem to point to a gradual increase in recharge year-to-year. For seven out of eight of the drainage basins the indices of agreement varied from 0.62 - 0.96, indicating moderate to strong agreement. For the six drainage basins with indices of agreement below 0.90 the experimental recharge calculated using the water budget model developed in this study exceeded the predicted USGS recharge. That is, experimental recharge was higher than standard recharge. Kuli‘ou‘ou was the most dramatic example of this trend, producing an index of agreement of 0.17, indicating strong disagreement. This disagreement was largely a result of categorizing the period from February 2007 - November 2012 as a drought, which lowered the standard USGS annual recharge from 1.57 to 0.51 $Mm^3\ y^{-1}$ (Table 3; Frazier et al., *in review*). Annual recharge for Kuli‘ou‘ou between June 2009 and September 2010 was $1.93 \pm 1.81\ Mm^3\ y^{-1}$ (Table 3). Changing the standard USGS recharge to reflect normal climate conditions during this period produces an agreement of 0.92, suggesting recharge was above average. In fact, for the five drainage basins that had the longest records (Mākaha, Kahana, Hālawa, Kaukonahua, and Opae Ula), there was an overall trend towards increased recharge between 1997 and 2014 (Figure 11). While the otherwise-strong agreement between experimental and standard recharge is a partial validation of the water budget model developed in this study, it is also a consequence of the large uncertainties propagated through the error calculations. The index of agreement describes how well predicted values fit within a range of uncertainty. The larger the range of uncertainty the stronger the agreement, a fact which emphasizes the importance of clearly communicating uncertainty throughout the scientific process, and of not overstating the accuracy of any model developed to describe natural processes.

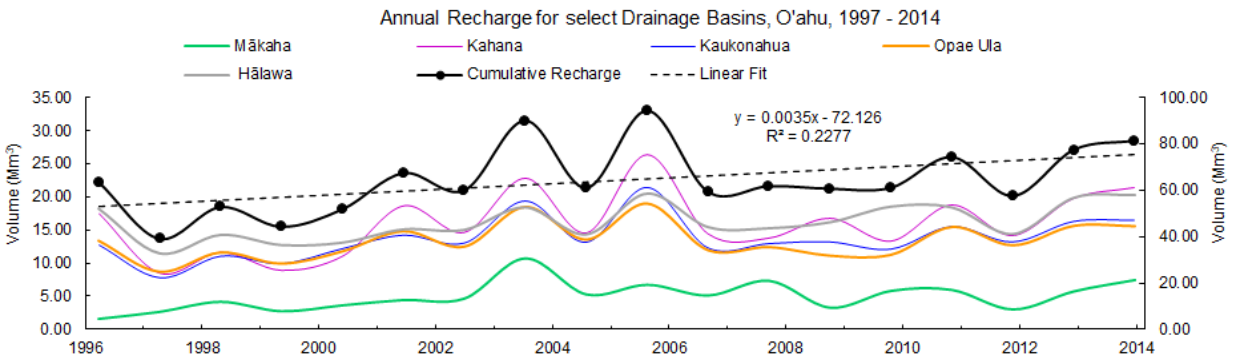

Figure 11. Cumulative annual recharge for five drainage basins on O‘ahu (Hālawa, Kaukonahua, Opae Ula, Kahana, and Mākaha) between 1997 and 2014 (right vertical axis), with individual drainage basin recharge overlaid (left vertical axis). A linear regression was completed on the cumulative infiltration estimates, with a positive slope of 0.0035, and an R2 = 0.23. The positive slope suggests a gradual increase in recharge.

3.5 Seasonality and Interannual Climate Variability

Recharge estimates show a strong response to seasonality and interannual climate variability lending additional weight to the good agreement with USGS recharge estimates. All drainage basins show a clear seasonal effect on precipitation, QF and recharge, with higher estimates during wet seasons and lower estimates during dry seasons. This pattern is especially pronounced for the Mākaha drainage basin, which shows strong seasonal oscillation through most of the period considered (Figure 12). However, across most drainage basins there are irregular departures from, and exaggerations to, this pattern, which loosely correspond to periods of drought and/or El Niño-Southern Oscillation (ENSO) events.

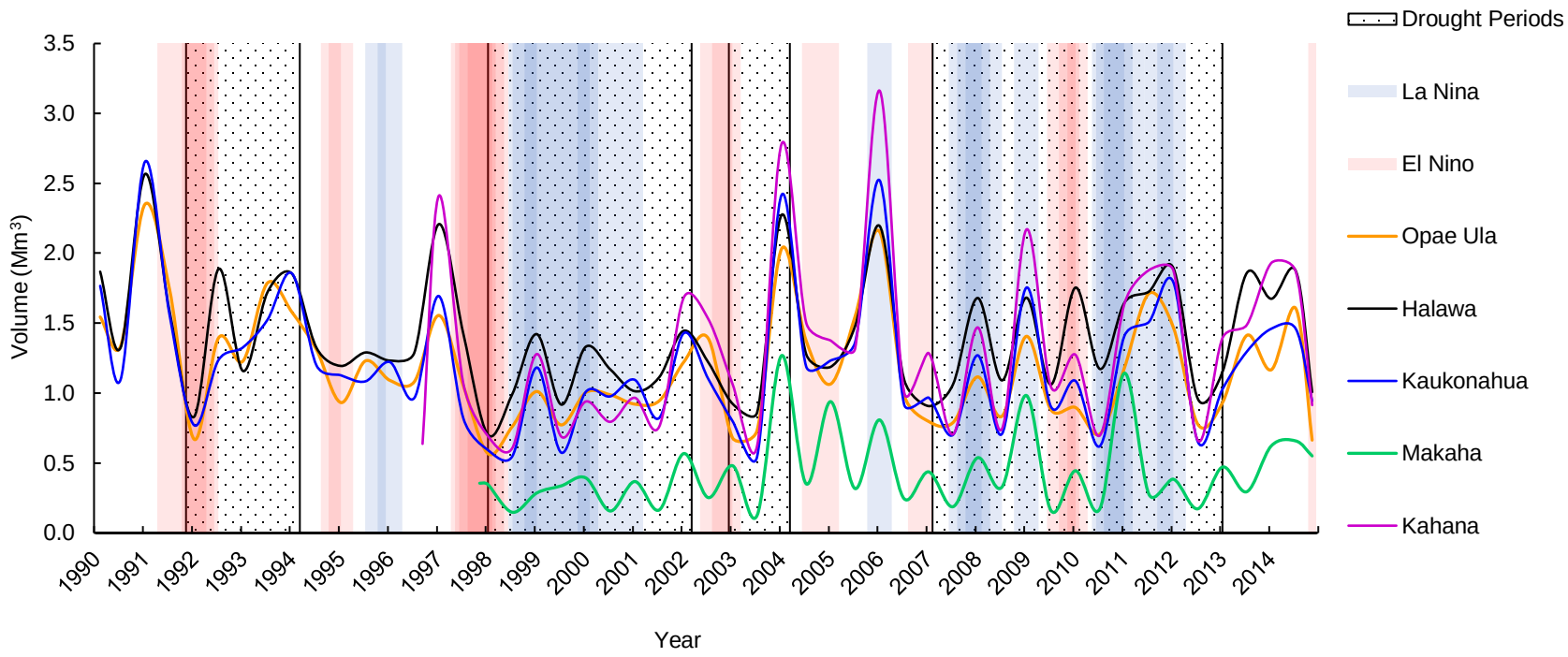

Figure 12. Seasonal recharge for five drainage basins on the island of Oʻahu, Hawaiʻi, 1990 - 2014, calculated using daily rainfall and temperature maps from Longman et al. (2019). Historical periods of drought from Frazier et al. (*in review*) and El Niño-Southern Oscillation (ENSO) events (NOAA, 2001) are overlaid. ENSO events were determined using the Oceanic Niño Indix (ONI). The ENSO color gradients reflect the severity of the event. Darker colors represent higher sea surface temperature (SST) anomalies by increments of ± 0.5˚C from mean SST.

Droughts are a regular part of Hawai‘i’s climate cycle (Frazier et al., *in review*), but recent research indicates drying trends across much of the state could increase the frequency and severity of droughts (Timm et al., 2015; McKenzie et al. 2019; Frazier & Giambelluca, 2017). Droughts in Hawai‘i have been associated with ENSO events. The warm phases (El Niño events) tend to bring heavy summer rainfall followed by abnormally dry winters (Chu, 1989; Chu & Chen, 2005; Frazier et al., 2018). The cool phases of the ENSO cycle (La Niña) have the opposite effect, bringing drier summers and wetter winters (Chu & Chen, 2005; Diaz & Giambelluca, 2012). There are four extreme droughts in the study period: Mar. 2007 - Dec. 2012, Feb. 1998 - Feb. 2002, Jan. 2003 - Feb. 2004, and Dec. 1991 - Feb. 1994 (Frazier et al., *in review*). These correspond well with several periods of low seasonal recharge and precipitation across O‘ahu (Figure 12). Seasonal water budgets also reflect ENSO events, notably the wet seasons of 1991-1992, 1994-1995, 1997-1998, 2002-2003, & 2006-2007 and the dry seasons of 1998, and 1999 (Figure 12). Despite some irregularities, interannual climate trends show that the recharge estimates derived from the water budget model developed in this study behave as expected through most years, while maintaining long-term averages close to standard recharge.

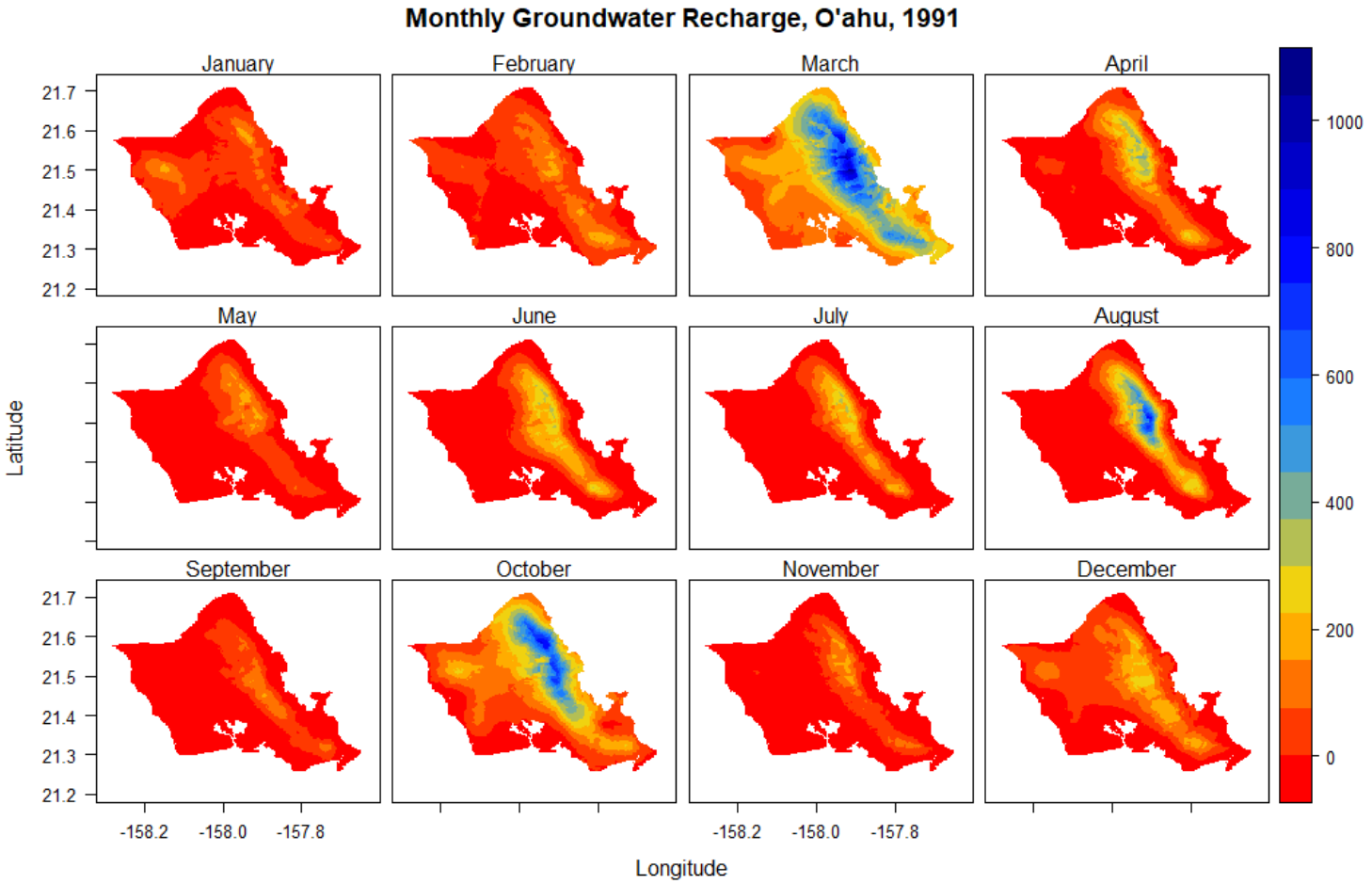

Figure 13. Monthly recharge for the island of O‘ahu in 1991. Maps were generated using a simplified water budget model: recharge ≈ precipitation - quickflow - evapotranspiration. Monthly precipitation estimates were derived from the daily rainfall maps of Longman et al. (2020). Monthly quickflow was estimated using runoff coefficients given in Engott et al. (2015). Monthly evapotranspiration was estimated by using the daily temperature maps from Longman et al. (2020) as inputs to a modified version of the Thornthwaite equation for potential evapotranspiration (PET). PET was converted to actual evapotranspiration (AET) by limiting PET to the moisture available from precipitation.

4. Conclusion

Daily precipitation and temperature maps were used to calculate monthly groundwater recharge for the island of O'ahu between 1990 and 2014 with a simplified water budget model. To assess the accuracy of this model, standard and experimental water budget components were calculated in eight drainage basins across the island. Uncertainties derived from experimental and standard values were propagated through the recharge calculations to produce a range of annual recharge uncertainty, which was then used to compare annual experimental recharge estimates with annual long-term average recharge calculated by the USGS (Engott et al. 2015). Experimental recharge estimates derived from this model agree strongly with the USGS recharge. Interannual climate trends further corroborated this agreement. These findings indicate that monthly estimates of groundwater recharge may be produced on Oʻahu via a low data intensity method with sufficient accuracy to better constrain current and historical recharge patterns for the island (Figure 13; Appendix C). They also suggest that the model presented here may be more broadly applicable to areas where atmospheric and runoff data are available. Since experimental recharge was calculated using monthly temperature and precipitation raster data and seasonal QF estimates, this technique can be replicated at any point where those data are available, or over any area where there is a sufficient density of point data to allow interpolation. Anticipating the future publication of near real-time daily temperature and precipitation maps for the State of Hawaiʻi, it may be possible to estimate monthly recharge in near real-time across the state. Temporally refined recharge estimates have potential to improve the accuracy of geochemical methods used to understand the movement and distribution of groundwater, such as tracer and mass balance studies, and could greatly aid water resource managers in their efforts to sustain and protect freshwater resources, both in Hawaiʻi and elsewhere.

Funding

This project has been funded by the NSF Hawaiʻi EPSCoR Program through the National Science Foundation's Research Infrastructure Improvement award (RII) Track-1: 'Ike Wai: Securing Hawaiʻi's Water Future Award # OIA-1557349. G.T. is supported by NSF Grant AGS-1945972. The project was also funded by the Department of Defense (DoD) Science, Mathematics and Research for Transformation (SMART) Service-for-Scholarship program. The views expressed are those of the author and do not necessarily reflect the views of any of the agencies listed.

Appendix A: **Baseflow Separation Supplementary Material**

Quickflow and baseflow can be differentiated on a stream hydrograph through a process called baseflow separation. In a simplified sense, this can be thought of as connecting the troughs on a stream hydrograph (Figure 5). Baseflow is determined by isolating the low flow points and interpolating baseflow values between these local minima. Many variations to this general technique exist, varying in both how local minima are determined and how the baseflow is interpolated (Institute of Hydrology, 1980; Piggott et al., 2005; Aksoy et al., 2008, 2009; Wahl & Wahl, 1995). One of the most widely used techniques was developed by Wahl & Wahl (1995) and uses sequential fixed windows to determine local minima and then conditionally assigns those minima as baseflow. The total hydrograph is divided into fixed blocks, the minimum streamflow from each block is identified and then assigned as baseflow if a fraction of the minimum exceeds adjacent minima. This technique requires two parameters which vary regionally: the size of the fixed block, and a turning point test factor. The turning point test factor is a number between zero and one and is used to determine the minima fraction for comparison. In Hawai‘i five-day blocks and a turning point test factor of 0.9 are used (Engott et al. 2015). Once all baseflow days have been assigned, intervening baseflow is linearly interpolated. This technique has been used by the USGS in several Hawai‘i applications (Izuka et al. 2005; Engott & Vana, 2007; Engott, 2011; Engott et al. 2015), and has been shown to provide reasonable estimates of baseflow and, therefore, quickflow.

For comparison with the general “fixed-window” technique used by the USGS an additional baseflow separation was completed using an alternative technique developed by Koskelo et al. (2012) called the sliding-average with rainfall record (SARR). The SARR baseflow separation is another smoothed minima technique modified from the United Kingdom Institute of Hydrology (UKIH) method (IH, 1980; Gustard et al., 1992). The SARR, UKIH and Wahl & Wahl (1995) techniques are all similar in that they compare adjacent daily streamflow measurements to determine local minima and then linearly interpolate baseflow based on those minima. The SARR technique stands out in two respects. First, whereas most baseflow separation techniques use sequential fixed windows to compare minima and identify baseflow days, the SARR technique employs a sliding window with three 2-day blocks to compare mean discharge between each block. The mean discharge in each 2-day block is compared, and baseflow is assigned to the first day of the middle block if 90% of the mean discharge in the

middle block is less than the mean discharge from the adjacent blocks. If the mean discharge in adjacent blocks exceeds 90% of the mean discharge in the middle block, then baseflow is assigned by linear interpolation from adjacent baseflow days. This is an improvement on techniques using sequential fixed windows in that it does not automatically discard streamflow measurements within a block that exceed the minimum, which amounts to 80% of points when using a 5-day fixed window - i.e., 4 out of 5 points in a 5-day window are not the minima and are, therefore, discarded. Use of the sliding 2-day window allows the SARR baseflow separation to better capture quick stream responses to precipitation events in small flashy catchments, like those of the Hawaiian Islands (Engott et al. 2015; Shade & Hunt 1996; Hawaii Water Authority 1959). The second major modification of the SARR baseflow technique is the incorporation of daily precipitation data. This is a "quality control procedure" added by the SARR developers to ensure a quickflow response is preceded by a precipitation event within the previous 1 or 2 days (Koskelo et al., 2012, pp 269). When the precipitation rule is violated, all stream discharge is considered baseflow. This protects the output of the baseflow separation from the effects of irrigation or other man-made groundwater input and is potentially unique to the SARR technique (Koskelo et al., 2012).

Appendix B: Opae Ula Drainage Basin Water Budget Sample Code

The code below was prepared in RStudio (RStudio Team 2021). Code chunks are displayed within the light gray boxes.

1. Load and Prepare Data

Stream data can be found at https://waterdata.usgs.gov/hi/nwis/uv?site_no=16211600.

30-year average monthly precipitation and evapotranspiration maps are available on the Rainfall Atlas of Hawai‘i at http://rainfall.geography.hawaii.edu/

USGS recharge maps for Hawai‘i are available at https://pubs.er.usgs.gov/publication/sir20155010 as shapefiles. These were converted to rasters using the Polygon to Raster function in ESRI's Conversion toolset in ArcMap and are available upon request.

```
# Load the Oahu recharge map from Engott et al. 2015
# Units are inches per year
oahu_rech   <- raster("oahu_rech")    # Average climate conditions
oahu_rech_d <- raster("oarech_drght") # Drought climate conditions
```

Daily rainfall maps for O‘ahu from 1/1/1990 - 12/31/2014 are available at https://waihona.its.hawaii.edu/index.php/s/8BMnWSC6LwXKfQ3. These were sorted manually into raster stacks for use in the baseflow separations.

Aquifer boundaries for Hawai‘i are available on the State of Hawai‘i GIS portal at https://planning.hawaii.gov/gis/download-gis-data/. Drainage basin boundaries were derived using ESRI's Hydrology toolset in ArcMap and are available upon request.

```
# Load shapefile containing dimensions of the drainage basin
db_opa <- readOGR(dsn = ".", layer = "db_opaeula")
```

The raster maps were sampled using the drainage basin and aquifer shapefiles with the cellStats() and mask() functions in the R package "raster". The daily rainfall raster stacks were sampled with the same functions using a loop. Only the first 6 months of the daily rainfall maps have been included here to reduce processing time. The coordinate reference system of the rainfall maps has also been reprojected from lat/long to Universal Transverse Mercator (UTM) to match the drainage basin shapefiles.

```
# Load the rainfall maps
rastlist <- list.files(path = ".",
                       pattern = '.tif$',
                       all.files = FALSE,
                       full.names = FALSE)
# Create raster stack
allrasters <- stack(rastlist)
# Clip all the maps to the drainage basin dimensions
allrasters <- mask(allrasters, db_opa) # This may take several minutes to run
```

Now the daily rainfall rasters are sorted by month.

```
sep97 <- allrasters[[1:30]]
oct97 <- allrasters[[31:61]]
nov97 <- allrasters[[62:91]]
dec97 <- allrasters[[92:122]]
jan98 <- allrasters[[123:153]]
feb98 <- allrasters[[154:181]]
```

The loop below takes the stack of clipped daily rasters for each month and figuratively lays them on top of one another summing all the pixels stacked on top of one another. This produces a monthly total map where each pixel is the sum of all pixels for that month. This monthly total map is then averaged with the cellStats() function to provide a total monthly point precipitation estimate. Total monthly point precipitation is then converted to volume by multiplication with the drainage basin area.

```
# Determine mean monthly precipitation in drainage basins for water budgets
# List to loop over
raster_months <- list(sep97, oct97, nov97, dec97, jan98, feb98)
# Bin for loop
rain_opa  <- matrix(NA, nrow = length(raster_months), ncol = 1)
dates_opa <- seq(from = as.Date("9/1/1997",  format = "%m/%d/%Y"),
                 to = as.Date("2/28/1998", format = "%m/%d/%Y"),
                 "months")
for(i in 1:length(raster_months)){
  rain_opa[i,1] <- sum(cellStats(raster_months[[i]], stat = 'mean'))}
opa_monthly_precip <- data.frame(rain_opa, dates_opa)
# Convert mm to cubic meters
area_opa <- 7814933 # Opae Ula area (square meters)
opa_monthly_precip$rain_m3 <- opa_monthly_precip$rain_opa * area_opa / 1000
```

The loop below follows a similar procedure as the previous but creates a list of mean daily point precipitation estimates for the drainage basin.

```
# Determine mean daily precipitation in drainage basins for baseflow separations
days_opa <- seq(from = as.Date("9/1/1997",  format = "%m/%d/%Y"),
                to   = as.Date("2/28/1998", format = "%m/%d/%Y"),
                "day")
# Bin for loop
opa_daily <- vector(mode = "numeric", length = length(days_opa))
for(i in 1:length(opa_daily)){
  opa_daily[i] <- cellStats(allrasters[[i]], stat = 'mean')}
opa_daily_precip <- data.frame(days_opa, opa_daily)
```

Monthly temperature and rainfall maps are aggregated from the daily maps of Longman et al. (2020) and are available upon request.

```
# Mean monthly temperature maps for 1997 & 1998 are in the folder "Temp_Maps"
# Load the maps
path <- paste(getwd(), "Temp_Maps", sep = "/")
rastlist <- list.files(path = path,
                       pattern = '.tif$',
                       all.files = FALSE,
                       full.names = FALSE)
```

```
setwd(path)
temp_rasters <- stack(rastlist)

# Mean monthly rainfall maps for 1997 & 1998 are in the folder "RF_Maps"
# Load the  maps
path <- paste(getwd(), "RF_Maps", sep = "/")
rastlist <- list.files(path = path,
                       pattern = '.tif$',
                       all.files = FALSE,
                       full.names = FALSE)
setwd(path)
rf_rasters <- stack(rastlist)
```

Long-term average evapotranspiration maps are taken from the Rainfall Atlas of Hawai'i (Giambelluca et al. 2013).

```
# LTA-AET maps for Sep - Feb are located in the folder "LTA_AET"
path <- paste(getwd(), "LTA_AET", sep = "/")
setwd(path)
aet_jan <- raster("aet_mm_jan")
aet_feb <- raster("aet_mm_feb")
aet_sep <- raster("aet_mm_sep")
aet_oct <- raster("aet_mm_oct")
aet_nov <- raster("aet_mm_nov")
aet_dec <- raster("aet_mm_dec")
```

2. Determine Experimental Quickflow

Stream hydrograph baseflow separations were completed using continuous daily stream flow and precipitation data. The first baseflow separation below uses fixed five-day windows following Wahl & Wahl (1995). The inputs to the baseflow separation function are daily stream discharge measurements, the size of the sequential block (*n*), and the turning point test factor (*f*). The USGS used a block size of $n = 5\ days$, and a turning point test factor of $f = 0.9$.

```
# Fixed five-day window (FFW) baseflow separation
bfs <- function(fulldata, n, f){
# Determine the minima in sequential "n"-day blocks for comparison
  for(i in seq(from = 1, to = nrow(fulldata)-n, by = n)){
    fulldata[i,4] <- min(fulldata[i+1,2],
                         fulldata[i+2,2],
                         fulldata[i+3,2],
                         fulldata[i+4,2])
# Use turning-point test factor artificially reduce minimum discharge over each
# "n"-day block
    fulldata[i,5] <- f * fulldata[i,4]}
# Create new data frame without the intervening days between block start dates
  partdata <- na.omit(fulldata)
  for(i in 1:nrow(partdata)){
# Add column for minimum flow in previous block
    partdata[i+1,6] <- partdata[i,4]
# Add column for minimum flow in subsequent block
    partdata[i+1,7] <- partdata[i+2,4]}
# Remove first two lines without m-1 and m+1
  partdata <- na.omit(partdata)
```

```
# Compare adjacent blocks with modified minimum
# Assign value of -1 to blocks with no baseflow
  for(i in 1:nrow(partdata)){
    if(partdata[i,5] < partdata[i,6] &
       partdata[i,5] < partdata[i,7]){partdata[i,8] <- partdata[i,4]}
    else{partdata[i,8] <- -1}}
# Proper names for data frame columns
  colnames(partdata) <- c("day",
                          "discharge_cms",
                          "precip_m",
                          "min_flow_cms",
                          "tp_flow_cms",
                          "m-1_flow",
                          "m+1_flow",
                          "baseflow_cms")
# Identify the dates where storms/quickflow does NOT occur
  no_storms <- subset(partdata, baseflow_cms != -1)
# Interpolate baseflow values during storm events
  interp_bf <- data.frame(approx(no_storms$day, no_storms$baseflow_cms,
                                 xout = fulldata$day,
                                 rule = 2,
                                 method = "linear",
                                 ties = mean))
# Add interpolated baseflow values to data frame
  fulldata$interp_bf <- interp_bf$y
# Remove extra columns from data frame
  fulldata <- fulldata[,c(1,2,3,6)]
# Constrain interpolated baseflow to total measured discharge
  for(i in 1:nrow(fulldata)){
    if(fulldata[i,4] > fulldata[i,2]){fulldata[i,4] = fulldata[i,2]}
  }
# Add column for year
  fulldata[, "year"] <- format(fulldata[,"day"], "%Y")
  return(fulldata)
}
```

The baseflow separation below is the Sliding Average with Rainfall Record (SARR) and uses sliding two-day windows following Koskelo et al. (2012). The inputs to the baseflow separation are daily stream discharge data daily precipitation estimates and the turning point test factor (f = *0.9*).

```
# Sliding average with rainfall record (SARR) baesflow separation
sarr <- function(fulldata, f){
# The loop below calculates the values to compare to flow on day i
# in order to determine if a quickflow event has occurred.
# Three new columns are added (4,5,& 6)
# Select the column with the mean stream flow data (column 2 in Makaha dataset)
  for(i in 3:nrow(fulldata)-3){
    fulldata[i,4] <- f * min(fulldata[i,2], fulldata[i+1,2])
    fulldata[i,5] <- min(fulldata[i-1,2], fulldata[i-2,2])
    fulldata[i,6] <- min(fulldata[i+2,2], fulldata[i+3,2])}
  fulldata <- na.omit(fulldata) # Remove rows with NAs generated by loop
# The loops below identifies storm/quickflow events with the value of '1'
# by comparing sliding average baseflow values.
```

```
  for(i in 1:nrow(fulldata)-1){
    fulldata[i,7] <- mean(fulldata[i,2], fulldata[i+1,2])}
  fulldata <- na.omit(fulldata)
  for(i in 1:nrow(fulldata)){
    if(fulldata[i,4] > fulldata[i,5]){fulldata[i,7] <- -1}
    if(fulldata[i,4] > fulldata[i,6]){fulldata[i,7] <- -1}
    if(fulldata[i,7] > fulldata[i,2]){fulldata[i,7] <- fulldata[i,2]}}
# Reduce master matrix to date, flow, and sliding average baseflow
  fulldata <- fulldata[,c(1:3,7)]
# Proper names for columns
  colnames(fulldata) <- c("day",
                          "mean_discharge",
                          "precip_m",
                          "baseflow")
# Identify the dates where storms/quickflow does NOT occur
  no_storms <- subset(fulldata, baseflow != -1)
# Interpolate baseflow values during storm events
  interp_bf <- data.frame(approx(no_storms$day, no_storms$baseflow,
                                 xout = fulldata$day,
                                 rule = 2,
                                 method = "linear",
                                 ties = mean))
# Add interpolated baseflow values to data frame
  fulldata$interp_bf <- interp_bf$y
# Add estimates of quickflow to the master matrix
# If the interpolated baseflow is less than the measured mean discharge
# the quickflow is equal to the difference, otherwise the quickflow = 0
  for(i in 1:nrow(fulldata)){
    if(fulldata[i,5] < fulldata[i,2]){
      fulldata[i,6] <- fulldata[i,2] - fulldata[i,5]}
    else{fulldata[i,6] <- 0}}
  fulldata[,7] <- fulldata[,6]
# Reset quickflow values to 0 when no precipitation has occurred
# on that day and on previous day, and when no quickflow occurred
# on the previous day
  for(i in 2:nrow(fulldata)){
    if(fulldata[i,3] == 0 & fulldata[i-1,3] == 0 & fulldata[i,6] == 0){
      fulldata[i,7] = 0}}
# Repeat previous loop to eliminate erroneous quickflow events exceeding 1 day.
  for(i in 2:nrow(fulldata)){
    if(fulldata[i,3] == 0 & fulldata[i-1,3] == 0 & fulldata[i-1,7] == 0){
      fulldata[i,7] = 0}}
# Repeat again to eliminate residual erroneous quickflow events
  for(i in 2:nrow(fulldata)){
    if(fulldata[i,3] == 0 & fulldata[i-1,3] == 0 & fulldata[i-1,7] == 0){
      fulldata[i,7] = 0}}
# Create column for precipitation-adjusted sliding average baseflow
  for(i in 1:nrow(fulldata)){
    if(fulldata[i,7] == 0 & fulldata[i,5] > fulldata[i,2]){fulldata[i,8] =
       fulldata[i,2]}
    else{fulldata[i,8] = fulldata[i,5]}
    if(fulldata[i,6] > fulldata[i,7]){fulldata[i,8] = fulldata[i,2]}}
  mark <- 1
  for(i in 3:nrow(fulldata)){
    if(fulldata[i,7] == 0 & fulldata[i-1,7] > 0){mark = mark+1}
```

```
    else{mark = mark}
    fulldata[i,9] <- mark
    if(fulldata[i,7] == 0 & fulldata[i,3] == 0){fulldata[i,9] = 0}}
# Proper column names
  colnames(fulldata) <- c("day",
                          "mean_discharge",
                          "precip_m",
                          "baseflow",
                          "interp_bf",
                          "quickflow",
                          "quickflow_correct",
                          "bf_precip_correct",
                          "event_number")
  return(fulldata)
  }
```

Stream and precipitation data must be formatted correctly to be used as inputs in the baseflow separations as follows:

```
# Load stream and precipitation data
stream_opa             <- read.csv("Stream_Discharge_Opaeula.csv")
precip_opa             <- opa_daily_precip
# Convert to proper date format
stream_opa$datetime    <- as.Date(stream_opa$datetime, format = "%m/%d/%Y")
precip_opa$days_opa    <- as.Date(precip_opa$days_opa, format = "%Y-%m-%d")
# Clean up the data frames to only include dates, discharge and point precip columns
stream_opa             <- stream_opa[,c(3,4)] # Select discharge and date columns
precip_opa             <- precip_opa[,c(1,2)] # Select precip and date columns
# Convert all units to meters if needed
precip_opa$opa_daily   <- precip_opa$opa_daily / 1000 # Convert mm to m
stream_opa$discharge   <- stream_opa$discharge * 0.0283168 # Convert cfs to cms
# Make date columns match for merge() function
colnames(precip_opa)   <- c("day", "precip_m")
colnames(stream_opa)   <- c("day", "discharge_cms")
# Merge stream and precip data by date
fulldata_opa           <- merge(stream_opa, precip_opa, by = 'day', all = TRUE)
# Remove days without data
fulldata_opa           <- na.omit(fulldata_opa)

# Complete the baseflow separations
n <- 5 # Size of fixed blocks for Wahl & Wahl (1995) baseflow separation (days)
f <- 0.9 # Turning point test factor used by USGS for Oʻahu streams
# SARR baseflow separation
opa_sarr <- sarr(fulldata_opa, f)
# Fixed five-day window baseflow separation
opa_wahl <- bfs(fulldata_opa, n, f)
```

Plot the stream hydrograph with interpolated baseflow estimates.

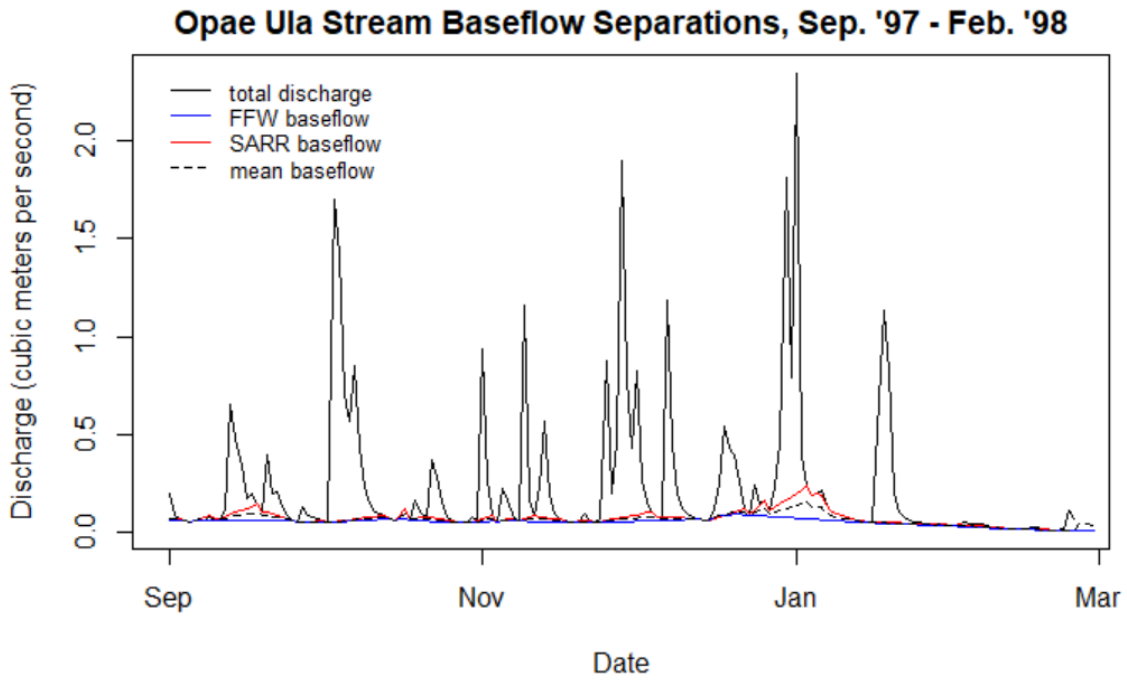


```
# Determine experimental monthly QF volume
# Add month column to daily baseflow separations
opa_sarr <- opa_sarr %>% mutate(month = month(day))
opa_wahl <- opa_wahl %>% mutate(month = month(day))
# Summarize data by month
opa_sarr_monthly <- opa_sarr %>%
  group_by(month) %>%
  summarise(qf_cms = sum(quickflow_correct))
opa_wahl_monthly <- opa_wahl %>%
  group_by(month) %>%
  summarise(interp_bf_cms = sum(interp_bf),
            discharge_cms = sum(discharge_cms))
# Column for quickflow for the FFW BFS
opa_wahl_monthly$qf_cms <- opa_wahl_monthly$discharge_cms - opa_wahl_monthly$interp_b
f_cms
# Columns for quickflow volume
opa_wahl_monthly$qf_m3  <- opa_wahl_monthly$qf_cms * 86400
opa_sarr_monthly$qf_m3  <- opa_sarr_monthly$qf_cms * 86400
# Mean monthly quickflow volume (m3)
print(mean_bfs_qf_m3    <- (opa_sarr_monthly$qf_m3 +
                              opa_wahl_monthly$qf_m3) / 2)

## [1] 492368.50  38308.01 215481.79 560203.71 671123.48 631803.42
```

3. Determine Standard Quickflow

Standard QF is taken directly from runoff coefficient maps in Engott et al. (2015, Figure 7). These maps were rasterized in ArcMap and are available upon request.

```r
# Determine standard QF for Opae Ula
# Pull runoff coefficients directly from Engott et al. (2015) Figure 7
RC_opa <- c(0.2, 0.2, 0.375, 0.375, 0.375, 0.375) # Two dry season, four wet season
print(stdr_qf_m3 <- opa_monthly_precip$rain_m3 * RC_opa)

## [1] 436097.7 210572.3 222440.9 707718.3 523737.5 581848.1
```

4. Determine Experimental Evapotranspiration

```r
# Calculate monthly precipitation-limited Thornthwaite AET
# First, calculate the Thornthwaite PET
# Create bin for loop
PET <- stack()
# Sequence through each year of temperature data
for(j in 1997:1998){
# Isolate temperature rasters by year
  temp_j <- raster::subset(temp_rasters,
                           grep(j, names(temp_rasters), value = T))
# Create bin inside the loop
  I_j <- stack()
# Sequence through each month within each year
  for(i in 1:12){
# Calculate heat index (I) for each year
    T_i <- (temp_j[[i]]/5)^1.514
    I_j <- stack(I_j, T_i)} # Close inner loop
  I_j <- calc(I_j, fun = sum, na.rm = T)
# Calculate alpha for each year
  alpha_j <- 0.49 + 0.0179 * I_j - 0.0000771 * I_j^2 + 0.000000675 * I_j^3
# Open another inner loop sequencing through each month
  for(i in 1:12){
# Calculate Thornthwaite PET using monthly temperature and annual heat index
    PET_i <- 1.6 * (10 * temp_j[[i]] / I_j)^alpha_j
# Collect each monthly PET map into the "PET" bin
    PET <- stack(PET, PET_i)}} # Close inner and outer loops
# Calculate the precipitation-limited Thornthwaite AET
# Convert monthly precip maps from mean to total monthly precip
months <- seq.Date(from = as.Date("1997-01-01", format = "%Y-%m-%d"),
                   to   = as.Date("1998-12-31", format = "%Y-%m-%d"),
                   by   = "month")
days <- days_in_month(months)
rf_rasters <- rf_rasters * days # Multiply mean monthly RF by number of days
# Convert PET from cm to mm
PET <- PET * 10
# Determine difference between Thornthwaite PET and RF
PLT_AET_neg <- PET - rf_rasters
# Eliminate all negative pixels
PLT_AET_neg[PLT_AET_neg < 0] <- 0
# Subtract difference between RF and PET from PET
PLT_AET <- PET - PLT_AET_neg # Precipitation-Limited Thornthwaite AET (mm/month)

# Add CRS to the PLT-AET maps
crs(PLT_AET)  <- "+proj=longlat +datum=WGS84 +no_defs"
# Reproject the drainage basin into the correct CRS
db_opa_latlon <- spTransform(db_opa, crs(PLT_AET))
# Extract monthly PLT-AET
PLT_AET_opa   <- cellStats(mask(PLT_AET, db_opa_latlon), stat = 'mean')
```

```r
# Select the Sep. 1997 - Feb. 1998
PLT_AET_opa   <- PLT_AET_opa[9:14]
# Convert from mm to cubic meters
print(PLT_AET_opa   <- PLT_AET_opa * area_opa / 1000)
```

5. Determine Standard Evapotranspiration

Standard ET was set as the long-term average AET from the Rainfall Atlas of Hawai'i

```r
# Extract Standard ET from the LTA AET maps
# Bin for loop
lta_aet       <- vector()
# Stack LTA AET maps
lta_aet_maps  <- stack(aet_sep, aet_oct, aet_nov, aet_dec, aet_jan, aet_feb)
# Loop to dete
for(i in 1:nlayers(lta_aet_maps)){
  lta_aet[i]  <- mean(cellStats(mask(lta_aet_maps[[i]], db_opa_latlon), stat = 'mean'
))}
# Convert to mm to m3
print(lta_aet <- lta_aet * area_opa / 1000)
```

```
## [1] 669930.4 612039.9 490691.6 476977.9 483151.3 472831.0
```

6. Determine Experimental Recharge

```r
# Determine monthly experimental recharge
# Recharge = precip - QF - ET
rech_ex <- as.numeric(opa_monthly_precip$rain_m3 - mean_bfs_qf_m3 - PLT_AET_opa)
# Get rid of negative recharge
rech_ex[rech_ex < 0] <- 0
rech_ex
```

```
## [1] 960450.2 323797.6      0.0 838342.5 229007.3 463144.6
```

7. Determine Standard Recharge

Standard recharge was determined by applying a monthly weighting factor to long-term average USGS recharge. The period between Sep. 1997 and Jan. 1998 is classified as a normal climate period. The month of Feb. 1998 marks the beginning of a statewide drought.

```r
# Extract Standard recharge from the LTA USGS recharge maps
stdr_rech   <- cellStats(mask(oahu_rech,   db_opa), stat = 'mean') # Normal climate
stdr_rech_d <- cellStats(mask(oahu_rech_d, db_opa), stat = 'mean') # Drought
# Convert from inches per year to m3 per 6 months
stdr_rech   <- stdr_rech   * 0.0254 * area_opa / 2
stdr_rech_d <- stdr_rech_d * 0.0254 * area_opa / 2
# Weight monthly recharge by precipitation volume
total_rf    <- sum(opa_monthly_precip$rain_m3) # Total precip Sep. 97 - Feb. 98
weight      <- opa_monthly_precip$rain_m3 / total_rf
stdr_rech   <- stdr_rech * weight
stdr_rech_d <- stdr_rech_d * weight
print(stdr_rech   <- c(stdr_rech[1:5], stdr_rech_d[6]))
```

```
## [1] 2099374.0 1013694.7  571109.6 1817042.8 1344678.4 1205960.5
```

8. Determine Recharge Uncertainty

Recharge uncertainty (δR) was determined by propagating error through the water budget calculations as follows:

$$\delta R = \sqrt{\delta P^2 + \delta QF^2 + \delta ET^2}$$

, where δP is precipitation uncertainty, δQF is quickflow uncertainty, and δET is evapotranspiration uncertainty. δP was taken directly from Longman et al. (2020) as 0.5 mm per pixel per day. δQF was set as the mean difference between standard and experimental QF. δAET was set as the mean difference between standard and experimental ET.

```
# Determine precipitation error
d_rf <- 0.5 * area_opa / 1000 # cubic meters
# Determine QF uncertainty
d_qf <- mean(abs(mean_bfs_qf_m3 - stdr_qf_m3)) # cubic meters
# Determine ET uncertainty
d_et <- mean(abs(lta_aet - PLT_AET_opa)) # cubic meters
# Determine recharge uncertainty
d_r  <- sqrt(d_rf^2 + d_qf^2 + d_et^2) / 10^6 # cubic meters
```

9. Results

Total recharge in the Opae Ula drainage basin between September 1997 and February 1998 was $2.81 \pm 0.63\ Mm^3$.

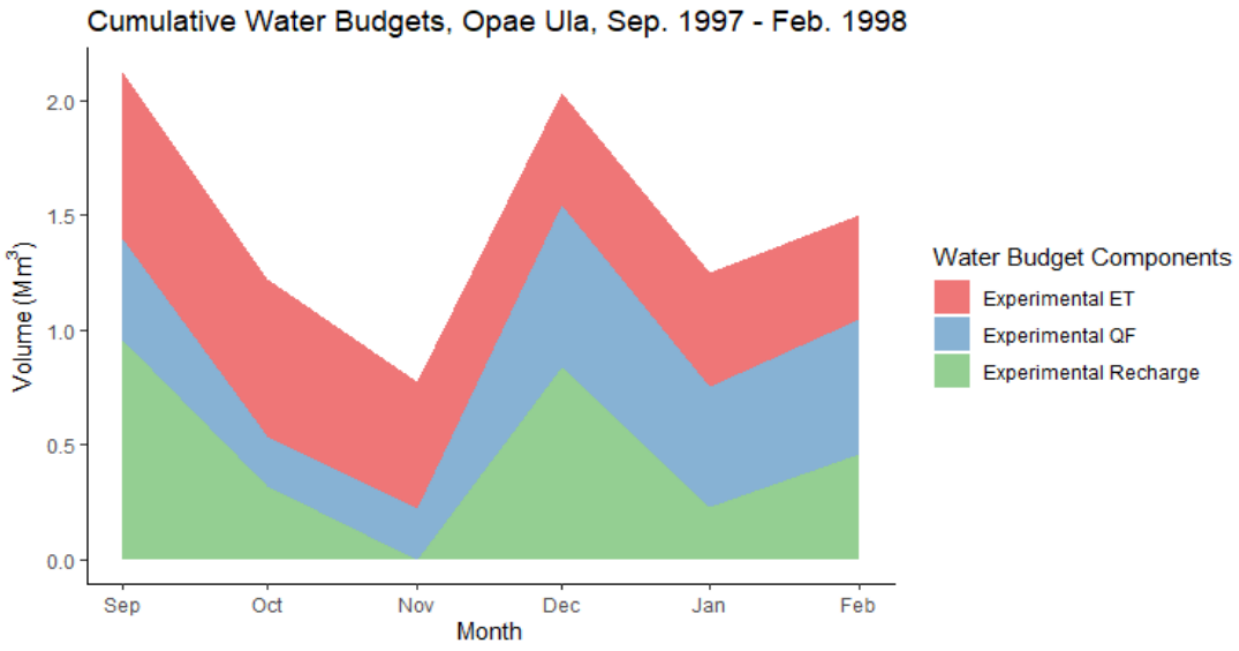

Appendix C: O'ahu Monthly Water Budgets Sample Code

The code below was prepared in RStudio (RStudio Team 2021).

```
# Load the rainfall maps
# Set path to location of the RF maps
rastlist <- list.files(path = "D:/RF_Oahu/Monthly_RF_Oahu",
                       pattern = '.tif$',
                       all.files = TRUE,
                       full.names = FALSE)
# Create raster stack
# Set working directory to location of the RF maps
setwd("D:/RF_Oahu/Monthly_RF_Oahu")
rf_rasters <- stack(rastlist)
# Assign CRS to each RF raster in the stack
for(i in 1:nlayers(rf_rasters)){
  proj4string(rf_rasters[[i]]) <- CRS("+proj=longlat +datum=WGS84")}

# Load the temperature maps
# Set path to the location of the temp maps
rastlist <- list.files(path = "D:/Temp_Oahu/Mean_Monthly_Temp",
                       pattern = '.tif$',
                       all.files = TRUE,
                       full.names = FALSE)
# Create raster stack
# Set working directory to the location of the temp maps
setwd("D:/Temp_Oahu/Mean_Monthly_Temp")
temp_rasters <- stack(rastlist)
# Assign CRS to each temperature raster in the stack
for(i in 1:nlayers(temp_rasters)){
  proj4string(temp_rasters[[i]]) <- CRS("+proj=longlat +datum=WGS84")}

# Calculate monthly precipitation-limited Thornthwaite AET
# First, calculate the Thornthwaite PET
# Create bin for loop
PET <- stack()
# Sequence through each year of temperature data
for(j in 1990:2014){
# Isolate temperature rasters by year
  temp_j <- raster::subset(temp_rasters,
                           grep(j, names(temp_rasters), value = T))
# Create bin inside the loop
  I_j <- stack()
# Sequence through each month within each year
  for(i in 1:12){
# Calculate heat index (I) for each year
    T_i <- (temp_j[[i]]/5)^1.514
    I_j <- stack(I_j, T_i)} # Close inner loop
  I_j <- calc(I_j, fun = sum, na.rm = T)
# Calculate alpha for each year
  alpha_j <- 0.49 + 0.0179 * I_j - 0.0000771 * I_j^2 + 0.000000675 * I_j^3
# Open another inner loop sequencing through each month
  for(i in 1:12){
# Calculate Thornthwaite PET using monthly temperature and annual heat index
```

```
    PET_i <- 1.6 * (10 * temp_j[[i]] / I_j)^alpha_j
# Collect each monthly PET map into the "PET" bin
    PET <- stack(PET, PET_i)}} # Close inner and outer loops
# Calculate the precipitation-limited Thornthwaite AET
# Convert monthly precip maps from mean to total monthly precip
months <- seq.Date(from = as.Date("1990-01-01", format = "%Y-%m-%d"),
                   to   = as.Date("2014-12-31", format = "%Y-%m-%d"),
                   by   = "month")
days <- days_in_month(months)
rf_rasters <- rf_rasters * days # Multiply mean monthly RF by number of days
# Convert PET from cm to mm
PET <- PET * 10
# Determine difference between Thornthwaite PET and RF
PLT_AET_neg <- PET - rf_rasters
# Eliminate all negative pixels
PLT_AET_neg[PLT_AET_neg < 0] <- 0
# Subtract difference between RF and PET from PET
PLT_AET <- PET - PLT_AET_neg # Precipitation-Limited Thornthwaite AET (mm/month)

# Determine quickflow for each month
# Load seasonal runoff coefficient maps modified from Engott et al. (2015)
RC_dry  <- raster("rc_dry")
RC_wet  <- raster("rc_wet")
# Create stack with monthly runoff coefficients
RC_wet1 <- stack(replicate(4, RC_wet)) # January - April
RC_dry  <- stack(replicate(6, RC_dry)) # May - October
RC_wet2 <- stack(replicate(2, RC_wet)) # November - December
RC      <- stack(RC_wet1, RC_dry, RC_wet2)
RC      <- stack(replicate(25, RC)) # Repeat for 25 years

# Determine Recharge for each month
QF <- rf_rasters * RC
R  <- rf_rasters - QF - PLT_AET
# Get rid of negative recharge pixels
R[R < 0] <- 0
# Proper names for the recharge maps
for(i in 1:length(months)){
  names(R)[i] <- paste("recharge", as.character(months[i]), sep = "_")}

# Plot (produces Figure 13)
R_1991 <- raster::subset(R, grep(1991, names(R), value = T))
cols <- colorRampPalette(colors = c("red", gold", "dodgerblue", "blue", "darkblue"))
levelplot(R_1991,
          main = "Monthly Recharge, O'ahu, 1991",
          col.regions = cols,
          names.attr = c("January", "February", "March", "April",
                         "May", "June", "July", "August",
                         "September", "October", "November", "December"),
          xlab = "Longitude",
          ylab = "Latitude")
```

References

Allen, R.G., Walter, I.A., Elliott, R.L., Howell, T.A., Itenfisu, D., Jensen, M.E., and Snyker, R.L. 2005. The ASCE Standardized Reference Evapotranspiration Equation. ASCE Library. https://doi.org/10.1061/9780784408056

Aksoy, H., Unal, N.E., Pektas, A.O., 2008. Smoother minima baseflow separation tool for perennial and intermittent streams. Hydrological Processes. 22 (22), 4467–4476.

Aksoy, H., Kurt, I., Eris, E., 2009. Filtered smoothed minima baseflow separation method. Journal of Hydrology. 372 (1–4), 94–101.

Bassiouni, M., & Oki, D. (2013). Trends and shifts in streamflow in Hawai‘i, 1913–2008. Hydrological Processes, 27(10), 1484–1500. https://doi.org/10.1002/hyp.9298

Bird, R.E. and Hulstrom, R.L. 1981. A Simplified Clear Sky Model for Direct and Diffuse Insolation on Horizontal Surfaces. Solar Energy Research Institute. https://instesre.org/Solar/BirdModelNew.htm

Booth, H., Lautze, N., Tachera, D., & Dores, D. (2021). Event-Based Stable Isotope Analysis of Precipitation Along a High Resolution Transect on the South Face of O'ahu, Hawai'i. Pacific Science 75(3), 421-441. https://www.muse.jhu.edu/article/805234.

Chu, P., & Chen, H. (2005). Interannual and Interdecadal Rainfall Variations in the Hawaiian Islands. Journal of Climate, 18(22), 4796–4813. https://doi.org/10.1175/JCLI3578.1

Chu, P. (1989). Hawaiian drought and the Southern Oscillation. Journal of Climatology, 9(6), 619–631.

Dores, D., Glenn, C., Torri, G., Whittier, R., & Popp, B. (2020). Implications for groundwater recharge from stable isotopic composition of precipitation in Hawai’i during the 2017–2018 La Niña. Hydrological Processes, 34(24), 4675–4696. https://doi.org/10.1002/hyp.13907

Dunne, T., & Leopold, L. (1978). Water in Environmental Planning. W.H. Freeman and Co.,San Francisco, CA.

Ekern, P. (1983). Measured Evaporation in High Rainfall Areas, Leeward Ko’olau Ranges, O’ahu, Hawai’i. Water Resources Research Center, University of Hawaii at Manoa.

Engott, J.A., 2011, A water-budget model and assessment of groundwater recharge for the Island of Hawai‘i: U.S. Geological Survey Scientific Investigations Report 2011–5078, 53 p.

Engott, J., Johnson, A., Bassiouni, M., Izuka, S., & Engott, J. (2015). Spatially distributed groundwater recharge for 2010 land cover estimated using a water-budget model for the island of O’ahu, Hawaii. Scientific Investigations Report. United States Geological Survey, 2015-5010. https://doi.org/10.3133/sir20155010

Engott, J.A., and Vana, T.T., 2007, Effects of agricultural land use changes and rainfall on round-water recharge in central and west Maui, Hawai‘i, 1926–2004: U.S. Geological Survey Scientific Investigations Report 2007–5103, 56 p.
Fackrell, J. (2016). Geochemical Evolution of Hawaiian Groundwater. [Honolulu] : [University of Hawaii at Manoa], [August 2016].

Frazier, A. G., and Giambelluca, T. W. (2017), Spatial trend analysis of Hawaiian rainfall from 1920 to 2012. International Journal of Climatology, 37(5), 2522–2531. https://doi.org/10.1002/joc.4862

Frazier, A.G., et al. (in review), A Century of Spatial and Temporal Patterns of Drought in Hawai'i across Hydrological, Ecological, and Socioeconomic Scales. Manuscript submitted for publication.

Frazier, A. G., Giambelluca, T. W., Diaz, H. F. and Needham, H. L. (2016), Comparison of geostatistical approaches to spatially interpolate month-year rainfall for the Hawaiian Islands. International Journal of Climatology, 36(3), 1459-1470. https://doi.org/10.1002/joc.4437

Frazier, A.G., Timm, O., Giambelluca, T.W., Diaz, H. (2018). The influence of ENSO, PDO and PNA on secular rainfall variations in Hawai‘i. Climate Dynamics, 51(5), 2127–2140. https://doi.org/10.1007/s00382-017-4003-4

Giambelluca, T. (1983). Water balance of the Pearl Harbor-Honolulu Basin, Hawai‘i, 1946-1975. Water Resources Research Center, University of Hawaii at Manoa.

Giambelluca, T.W., Chen, Q., Frazier, A.G., Price, J.P., Chen, Y.-L., Chu, P.-S., Eischeid, J.K., and Delparte, D.M., 2013, Online Rainfall Atlas of Hawai‘i: Bulletin of the American Meteorological Society, v. 94, p. 313–316, https://doi.org/10.1175/BAMSD-11-00228.1 , at http://rainfall.geography.Hawaii.edu/.

Giambelluca, T.W., Shuai, Xiufu, Barnes, M.L., Alliss, R.J., Longman, R.J., Miura, Tomoaki, Chen, Qi, Frazier, A.G., Mudd, R.G., Cuo, Lan, and Businger, A.D., 2014, Evapotranspiration of Hawai‘i, final report: submitted to U.S. Army Corps of Engineers–Honolulu District and Commission on Water Resource Management, State of Hawai‘i, 178 p.

Gingerich, S.B., and Oki, D.S., 2000, Ground Water in Hawaii: U.S. Geological Survey, 6 p.

Glenn, C., Whittier, R., Dailer, M., Dulai, H., El-Kadi, A., Fackrell, J., Kelly, J., Waters, C., Sevadjian, J. (2013). "Lahaina Groundwater Tracer Study – Lahaina, Maui, Hawaii." Final Report prepared from the State of Hawaii Department of Health, the U.S. Environmental Protection Agency, and the U.S. Army Engineer Research and Development Center.

Gustard, A., Bullock, A., & Dixon, J. (1992). Low flow estimation in the United Kingdom. Report - Institute of Hydrology (United Kingdom), 108.

Hawaii Water Authority. (1959). Water resources in Hawaii. Hawaii Water Authority.

Institute of Hydrology, 1980. Low Flow Studies, Research Reports 1 and 3. Institute of Hydrology, Wallingford, Oxfordshire, UK.
Izuka, S., Oki, D., & Chen, C. (2005). Effects of irrigation and rainfall reduction on ground-water recharge in the Lihue Basin, Kauai, Hawaii. U.S. Geological Survey.

Izuka, S.K., Engott, J.A., Rotzoll, Kolja, Bassiouni, Maoya, Johnson, A.G., Miller, L.D., and Mair, Alan, 2018, Volcanic aquifers of Hawai‘i—Hydrogeology, water budgets, and conceptual models (ver. 2.0, March 2018): U.S. Geological Survey Scientific Investigations Report 2015-5164, 158 p., https://doi.org/10.3133/sir20155164.

Jasechko, S., Birks, S., Gleeson, T., Wada, Y., Fawcett, P., Sharp, Z., McDonnell, J., & Welker, J. (2014). The pronounced seasonality of global groundwater recharge. Water

Kendall, C., & McDonnell, J. (1999). Isotope Tracers in Catchment Hydrology. Elsevier Science & Technology.

Koskelo, A., Fisher, T., Utz, R., & Jordan, T. (2012). A new precipitation-based method of baseflow separation and event identification for small watersheds (<50km2). Journal of Hydrology, 450-451, 267–278. https://doi.org/10.1016/j.jhydrol.2012.04.055

Krushelnycky, P., Starr, F., Starr, K., Longman, R., Frazier, A., Loope, L., & Giambelluca, T. (2016). Change in trade wind inversion frequency implicated in the decline of an alpine plant. Climate Change Responses, 3(1). https://doi.org/10.1186/s40665-016-0015-2

Longman, R., Diaz, H., & Giambelluca, T. (2015). Sustained Increases in Lower-Tropospheric Subsidence over the Central Tropical North Pacific Drive a Decline in High-Elevation Rainfall in Hawaii. Journal of Climate, 28(22), 8743–8759. https://doi.org/10.1175/JCLI-D-15-0006.1

Longman, R., Frazier, A., Newman, A., Giambelluca, T., Schanzenbach, D., Kagawa-Viviani, A., Needham, H., Arnold, J., & Clark, M. (2019). High-Resolution Gridded Daily Rainfall and Temperature for the Hawaiian Islands (1990–2014). Journal of Hydrometeorology, 20(3), 489–508. https://doi.org/10.1175/JHM-D-18-0112.1

Longman, R., Elison Timm, O., Giambelluca, T., & Kaiser, L. (2021). A 20-year analysis of disturbance-driven rainfall on O’ahu, Hawai’i. Monthly Weather Review. https://doi.org/10.1175/MWR-D-20-0287.1

Mair, A. (2009). Effects of rainfall variability and groundwater pumping on streamflow in Upper Makaha Valley. University of Hawaii at Manoa.

Mair, A. (2010). Influence of groundwater pumping and rainfall spatio-temporal variation on streamflow. Journal of Hydrology (Amsterdam), 393(3), 287–308. https://doi.org/10.1016/j.jhydrol.2010.08.026

McKenzie, M., Giambelluca, T., Diaz, H. (2019). Temperature trends in Hawai‘i: A century of change, 1917–2016. International Journal of Climatology, 39(10), 3987–4001. https://doi.org/10.1002/joc.6053
Monteith, J., 1965. Evaporation and environment. In G.E. Fogg (ed.) Symposium of the Society for Experimental Biology, The State and Movement of Water in Living Organisms, Vol. 19, pp. 205-234, Academic Press, Inc., NY, USA.

Nichols, W., Shade, P., & Hunt, C. (1996). Summary of the Oahu, Hawaii, regional aquifer-system analysis . U.S. G.P.O.

NOAA Climate Prediction Center. (2001, Jan. 1). Cold & Warm Episodes by Season. US National Weather Service. https://origin.cpc.ncep.noaa.gov/products/analysis_monitoring/ensostuff/ONI_v5.php

Noguchi, Y. (1979). Deformation of Trees in Hawaii and its Relation to Wind. The Journal of Ecology, 67(2), 611–628. https://doi.org/10.2307/2259116

Penman, H. L. (1948). Natural Evaporation from Open Water, Bare Soil and Grass. Proceedings of the Royal Society of London. Series A, Mathematical and Physical Sciences, 193(1032), 120–145. https://doi.org/10.1098/rspa.1948.0037

Piggott, A. (2005). A revised approach to the UKIH method for the calculation of baseflow / Une approche améliorée de la méthode de l’UKIH pour le calcul de l’écoulement de base. Hydrological Sciences Journal, 50(5), 911. https://doi.org/10.1623/hysj.2005.50.5.911

RStudio Team (2020). RStudio: Integrated Development for R. RStudio, PBC, Boston, MA URL http://www.rstudio.com/.

Safeeq, M. (2012). Hydrologic effect of groundwater development in a small mountainous tropical watershed. Journal of Hydrology (Amsterdam), 428-429, 51–67. https://doi.org/10.1016/j.jhydrol.2012.01.023

Scholl, M. (1995). An isotope hydrology study of the Kilauea volcano area, Hawai’i. U.S. Geological Survey.

Scholl, M., Gingerich, S., & Tribble, G. (2002). The influence of microclimates and fog on stable isotope signatures used in interpretation of regional hydrology: East Maui, Hawaii. Journal of Hydrology (Amsterdam), 264(1), 170–184. https://doi.org/10.1016/S0022-1694(02)00073-2

Scholl, M., Giambelluca, T., Gingerich, S., Nullet, M., & Loope, L. (2007). Cloud water in windward and leeward mountain forests: The stable isotope signature of orographic cloud water. Water Resources Research, 43(12), W12411–n/a. https://doi.org/10.1029/2007WR006011

Scholl, M., Eugster, W., & Burkard, R. (2011). Understanding the role of fog in forest hydrology: stable isotopes as tools for determining input and partitioning of cloud water in montane forests. Hydrological Processes, 25(3), 353–366. https://doi.org/10.1002/hyp.7762

Shade, P. (1984). Hydrology and sediment transport, Moanalua Valley, Oahu, Hawaii. U.S. Geological Survey.
State of Hawai‘i. (2019). Water Resource Protection Plan 2019 Update: Report prepared by Townscape Inc. for the State of Hawai‘i, Commission on Water Resource Management at https://dlnr.hawaii.gov/cwrm/planning/hiwaterplan/wrpp/

Stearns, H.T. & Macdonald, A.G. 1946. Geology and ground-water resources of the Island of Maui, Hawaii. Hawaii Div. Hydrogr. Bull. 7, 344.

Tachera, D., Lautze, N., Torri, G., & Thomas, D. (2021). Characterization of the isotopic composition and bulk ion deposition of precipitation from Central to West Hawai‘i Island between 2017 and 2019. Journal of Hydrology. Regional Studies, 34, 100786–. https://doi.org/10.1016/j.ejrh.2021.100786

Timm, O., Giambelluca, T., & Diaz, H. (2015). Statistical downscaling of rainfall changes in Hawai‘i based on the CMIP5 global model projections. Journal of Geophysical Research. Atmospheres, 120(1), 92–112. https://doi.org/10.1002/2014JD022059

Visher, F., & Mink, J. (1964). Ground-water Resources in Southern Oahu, Hawaii . U.S. Geological Survey.

Wada, C., Bremer, L., Burnett, K., Trauernicht, C., Giambelluca, T., Mandle, L., Parsons, E., Weil, C., Kurashima, N., & Ticktin, T. (2017). Estimating Cost-Effectiveness of Hawaiian Dry Forest Restoration Using Spatial Changes in Water Yield and Landscape Flammability under Climate Change. Pacific Science, 71(4), 401–424. https://doi.org/10.2984/71.4.2

Wahl, K.L., Wahl, T.L., 1995. Determining the flow of Comal Springs at New Braunfels, Texas. In: Proceedings of Texas Water ‘95, a Component Conference of the First International Conference on Water Resource Engineering. American Society of Civil Engineers, San Antonio, Texas, pp. 77–86.

Ward, A., Trimble, S., Burckhard, S., & Lyon, J. (2017). Environmental Hydrology (Third edition.). CRC Press, Taylor & Francis Group.

Willmott, C., & Wicks, D. (1980). An Empirical Method for the Spatial Interpolation of Monthly Precipitation within California. Physical Geography, 1(1), 59–73. https://doi.org/10.1080/02723646.1980.10642189

Willmott, C. (1981). On the Validation of Models. Physical Geography, 2(2), 184–194. https://doi.org/10.1080/02723646.1981.10642213

Willmott, C. (1982a). On the Climatic Optimization of the Tilt and Azimuth of Flat-plate Solar Collectors. Solar Energy, 28(3), 205–216. https://doi.org/10.1016/0038-092X(82)90159-1

Willmott, C. (1982b). Some Comments on the Evaluation of Model Performance. Bulletin of the American Meteorological Society, 63(11), 1309–1313. https://doi.org/10.1175/1520-0477(1982)063

Yeung, C., & Fontaine, R. (2007). Natural and diverted low-flow duration discharges for streams affected by the Waiahole Ditch System, Windward Oahu, Hawaii (Version 1.0.). U.S. Geological Survey.